Title
Adjuvant therapy with probiotic bacteria increases in vivo survival and function of natural killer cells in humanized mice

Author
Topchyan, Paytsar

Publication Date
2016

Peer reviewed|Thesis/dissertation

UNIVERSITY OF CALIFORNIA

Los Angeles

Adjuvant therapy with probiotic bacteria increases in vivo survival and function of natural killer cells in humanized mice

A thesis submitted in partial satisfaction of the requirements of the degree Master of Science in Oral Biology

by

Paytsar Topchyan

2016

ABSTRACT OF THE THESIS

Adjuvant therapy with probiotic bacteria increases in vivo survival and function of natural killer cells in humanized mice

by

Paytsar Topchyan

Master of Science in Oral Biology

University of California, Los Angeles, 2016

Professor Anahid Jewett, Chair

Natural killer cells target and kill cancer stem cells (CSCs)/undifferentiated tumors, as well as healthy, non-transformed stem cells. Following selection, NK cells differentiate CSCs, via secreted and membrane-bound IFN-γ and TNF-α. Probiotic bacteria increase the cytokine secretion function of split anergized NK cells, causing significant induction of IFN-γ. Thus, treatment of NK cells with probiotic bacteria induces differentiation of CSCs. Additionally, probiotic bacteria, in combination with osteoclasts maintain and expand highly functional NK cells for a long period of time. This novel method of expanding a large number of highly functional NK cells may be a breakthrough strategy for adoptive NK immunotherapy. In this study, NK immunotherapy was studied in combination with supplementation of probiotic bacteria in the humanized mouse model. NK immunotherapy increased cytokine production in immune tissue of subjects, while probiotic supplementation further enhanced these effects, resulting in more differentiated tumors *in vivo*.

The thesis of Paytsar Topchyan is approved by

Ichiro Nishimura

Nicholas A. Cacalano

Anahid Jewett, Committee Chair

University of California, Los Angeles

2016

DEDICATION

This thesis is first and foremost dedicated to my hard-working parents, Vardan and Asmik Topchyan. I would not be where I am today without the sacrifices you have made, motivating me to seize every opportunity in life. There are no words to express how much I love and admire you. Thank you for giving me the world!

TABLE OF CONTENTS

I. **Abstract**……..ii

II. **Committee page** ……iii

III. **Dedication**…….…….iv

IV. **Acknowledgement**…….....vi

V. **Introduction** ……...1

VI. **Thesis Outline**…….7

VII. **Materials and Methods**…….…….8

VIII. **Chapter 1: Specific Aim 1**……16

IX. **Chapter 2: Specific Aim 2**……26

X. **Chapter 3: Specific Aim 3**……33

XI. **Discussion**…….…….60

XII. **Final Conclusion**…….…….64

XIII. **References**…….……...65

ACKNOWLEDGEMENTS

I would like to acknowledge all of my lab mates who have been my mentors, confidantes, colleagues and friends. You have taught me so much!

Most importantly, I would also like to acknowledge and thank my mentor, Dr. Anahid Jewett, for her guidance and support. I could not have asked for a more intelligent and caring mentor. Thank you for being such an incredible role model and for instilling in me a drive to always strive for more.

INTRODUCTION

Natural killer cells

Natural killer (NK) cells are immune cells that develop in the bone marrow and constitute about 5-10% of lymphocytes in the peripheral blood and secondary lymphoid organs [1]. NK cell effector functions include direct cytotoxicity, antibody-dependent cellular cytotoxicity (ADCC), and inflammatory cytokine and chemokine secretion. These secreted factors indirectly regulate other immune cells' functions [2, 3]. NK cells mediate cytotoxicity against both transformed cells and healthy cells by releasing perforin and granzyme B, pre-formed granules of proteins. These proteins can induce apoptosis of target cells [4-6]. NK cells target and kill cancer stem cells (CSCs)/undifferentiated tumors, as well as healthy, non-transformed stem cells, which express low levels of major histocompatibility complex class I (MHC-I), CD54 and B7H1, and high levels of CD44 [7, 8].

In the past, our laboratory has shown, that following selection (NK cell-mediated lysis) of stem-like tumors, NK cells differentiate CSCs, otherwise known as undifferentiated or poorly differentiated tumors, via secreted and membrane-bound IFN-γ and TNF-α. This leads to tumor growth prevention and tumor microenvironment remodeling [9]. Activating receptors and co-receptors that recognize ligands expressed on tumors or virus-infected cells are responsible for mediating NK cell activation [10, 11]. Medium/high cytotoxic activity of lymphocytes in the peripheral blood is associated with a reduced cancer risk, and a high level of NK cell infiltration within the tumor is associated with better prognosis [11, 12]. On the other hand, low cytotoxic activity is associated with increased cancer risk [13]. The number of NK cells, along with their cytotoxic and cytokine secreting functions were significantly diminished in cancer patients [13-22].

Split anergy in NK cells

Our laboratory coined the term 'split anergy,' to indicate reduced NK cell cytotoxicity in the presence of significant secretion of cytokines [8, 23, 24]. Induction of split anergy in NK cells promotes differentiation of target cells via secreted and membrane-bound factors, increases key differentiation receptors on tumor cells, induces tumor cell resistance to NK cell-mediated cytotoxicity, and inhibits inflammation due to a decrease or shutdown of cytokine and chemokine production after tumor differentiation.

Probiotic bacteria

In the early 20th century, Elie Metchnikoff discovered that certain strains of bacteria in the human gut were beneficial to gut homeostasis; these beneficial bacteria were named probiotics [25]. Probiotics are commonly used in foods and supplements in an effort to enhance the innate immune system, including NK cells activity, and maintain the digestive tract's microbial balance [26-28]. The majority of probiotics consist of lactic-acid producing bacteria, including *lactobacilli, streptococci,* and *bifidobacteria*. The wide range of benefits observed with the use of probiotic bacteria suggests their integral role in the modulation of local gut immunity, as well as systemic immunity [29-31]. These beneficial bacteria effect production of immunoglobulin A [31-33], stimulate macrophages activity [34] and may reduce the effects of toxicity in anti-cancer therapy [35]. They also induce immature dendritic cells to differentiate into regulatory dendritic cells, induce the presence of regulatory T cells and increase NK cell activity, resulting in local intestinal defense [25, 27]. Areas of research pertaining to probiotic bacteria are fast-growing, with a promising outlook for treatment of medical conditions such as

gut mucosal pathologies, allergies, obesity, metabolic syndrome, heart disease, and cancer prevention or treatment, and so on [36-39].

Although the benefits and role of probiotics in immune modulation has been well known, the underlying mechanisms of NK cell immunomodulation is not understood. This study will provide, further information regarding the outcome of probiotics in regulating NK cell function. Probiotic bacteria induce significant split anergy in activated NK cells, leading to a significant induction of IFN-γ and TNF-α. In addition, probiotic bacteria induce significant expansion of NK cells [40] .

Osteoclasts

Osteoclasts are a type of bone cell, derived from hematopoietic stem cells. Their function, resorbing bone tissue, is critical for the maintenance, repair, and remodeling of bones. Bone homeostasis is achieved when there is a balance between osteoblast bone formation and osteoclast bone resorption [41]. Osteoclasts mature through stimulation from osteoblasts expressing RANKL, and their interaction, mediated by firm adhesion via ICAM-1[42]. Feng et al. [43] showed that osteoclasts also express many ligands for receptors present on activated NK cells. They reported that osteoclasts express ULBP-1, ULBP-2/5/6 and ULBP-3, but little or no MIC-A, MIC-B, or MHC class I-like ligands for NKG2D, the activating receptor of NK cells [44].

It was previously shown that osteoclasts, in comparison to dendritic cells and monocytes, are significant activators of NK cell expansion and function [40]. Additionally, osteoclasts secrete significant amounts of IL-12, IL-15, IFN-γ and IL-18, which are known to activate NK cells; osteoclasts also express important NK-activating ligands [40]. This study will provide a

novel strategy, discussing how to expand highly functional, osteoclast-expanded NK cells to levels that are significantly higher than those established by other methodologies (Specific Aim 2). Several *in vitro* NK expansion techniques have been developed to establish a higher therapeutic cell dosage, while boosting activity and *in vivo* proliferative potential of NK cells [45-60]. Some of these techniques include the stimulation of peripheral blood mononuclear cells (PBMCs), PBMC-purified populations of NK cells, or the use of human cord blood, sometimes in combination with various feeder cells such as K562 cells expressing membrane-bound IL-15 and 41BB ligand (K562-mb15-41BBL), EBV-TM-LCL, Wilm's tumor or irradiated PBMCs. These studies have generated clinically relevant NK cell numbers that have good function [52, 61, 62].

This study discusses a novel method to expand NK cells using osteoclasts, resulting in enhanced sensitization of tumor target cells to NK cell-mediated apoptosis, as well as cytokine production. This recent discoveries in NK expansion, to improve their effector functions against tumors, will be further discussed in the translational research conducted using humanized mice.

Humanized Mouse Model

Varying levels of NK cell impairment and/or deletion in nude, NOD-*scid* and NSG strains could explain discrepancies in the ability of CSCs to give rise to human tumors in these different immunodeficient strains [63]. Many questions have been raised, based on previous studies performed on immunodeficient animals, regarding specific immune subsets and their roles in controlling cancer initiation, growth, and metastasis. Since it is difficult to assess and compare the aggressiveness and metastatic potential of primitive CSCs using immunodeficient

mouse strains, humanized mice, with restored human immune systems, offer the most suitable platform to implant such tumors [64].

There have been numerous attempts to generate mice that bear a fully reconstituted human immune system. There are also differences between human immune system reconstitution levels supported by specific mouse strains. Since it is critical for the background strain to harbor severe immunodeficiency, NSG or NRG mice have typically been the strain of choice [65, 66]. There are many methods in creating various humanized mouse models, with differences in the age of mice, transplanted cell type, source or donor cell type, injection/implantation method, irradiation, etc. Of these variations, the simplest humanization method consists of injecting immunodeficient mice with human PBMCs, obtained from adult healthy donors/patients [67, 68]. PBMCs circulate in the blood, either dying or migrating to other tissues; the downside is that these mice can only be used for short term experiments, since circulating mature immune cells in mice initiate graft versus host disease (GvHD) against murine recipients [69].

Another method uses isolated $CD34^+$ progenitor cells originating from the peripheral blood, cord blood or fetal liver. $CD34^+$ cells are injected into either newly born or adult NSG mice. They stably engraft into the bone marrow and are capable of differentiating into all hematopoietic lineages of the human immune system. The CD34+ humanized mouse model's major limitation is that it lacks the presence of a human thymus; so instead, T cells undergo selection in the context of the mouse MHC [64, 70].

The BLT humanized mouse (hu-BLT) represents the most advanced and complete humanized mouse model generated, to date [70]. The human immune engraftment protocol consists of surgically implanting pieces of human fetal liver and thymus tissue under the renal capsule of NSG mice, followed by tail vein IV injection of same-donor $CD34^+$ hematopoietic

cells to support full reconstitution of the human bone marrow [64, 71, 72]. Thus, positive and negative selection of developing T cells occurs in the presence of human thymus. Consequently, immature T cells become functional $CD4^+$ helper and $CD8^+$ cytotoxic T cells after human MHC class I and class II restriction [70, 73]. The hu-BLT model is the only known humanized mouse model to displays mucosal immunity [74]. Hematopoietic stem cells (HSCs) develop, at least to some extent, into human T cells, B cells, NK cells, monocytes, myeloid derived suppressor cells (MDSCs), macrophages, dendritic cells, erythrocytes, and platelets in the BLT's tissues [75-78]. Long-term peripheral reconstitution of human $CD45^+$ immune cells is usually within the 30-80% range, as detected in the blood, spleen and bone marrow (manuscript in preparation). Human immune cells have been detected in the reproductive tract of females, intestines and rectum [79, 80], as well as the gingiva (manuscript in prep). It is also worth noting that NSG-BLT mice (BLT mice developed from NSG background strain) exhibit substantially higher levels of human leukocyte reconstitution in their peripheral blood than NOD-*scid*-BLT mice [74]. These features demonstrate that hu-BLT, developed from NSG background, is arguably the best available model for studying human immunity, thus far.

Purpose of Study

The purpose of this study is to investigate the role of probiotic bacteria as adjuvant therapy with NK immunotherapy to increase the survival and function of NK cells and their ability to target oral cancer stem cells in hu-BLT mice.

THESIS OUTLINE

Specific Aim 1: To investigate the role of probiotics in the activation of NK cells.

Specific Aim 2: To investigate the capability of osteoclasts in expanding NK cells in combination with probiotic bacteria.

Specific Aim 3: To investigate the use of adjuvant probiotic supplementation in combination with osteoclast-expanded NK immunotherapy in hu-BLT mice.

MATERIALS AND METHODS

Cell lines, reagents, and antibodies

Human immune cells were cultured in RPMI 1640, supplemented with 10% fetal bovine serum (FBS) (Gemini Bio-Products, CA). Oral squamous carcinoma stem cells (OSCSCs) were isolated from oral cancer patient tongue tumors at UCLA School of Medicine and cultured in RPMI 1640, supplemented 10% FBS (Gemini Bio-Products, CA), 1.4% antibiotic antimycotic, 1% sodium pyruvate, 1.4% MEM non-essential amino acids, 1% L-glutamine, 0.2% gentimicin (Gemini Bio-products, CA) and 0.15% sodium bicarbonate (Fisher Scientific, PA).

Antibodies to CD16 were purchased from Biolegend (San Diego, CA, USA). Recombinant IL-2 was obtained from NIH-BRB. Antibodies against isotype control, MHC-I, CD45 (human), CD45 (mouse), CD3, CD16, CD56, CD8, HLADR, and CD11b were purchased from Biolegend (San Diego, CA). Human NK purification kits were obtained from Stem Cell Technologies (Vancouver, BC, Canada).

Human monocytes/osteoclasts were cultured in alpha-MEM medium (Life Technologies, CA), supplemented with 10% FBS, and penicillin-streptomycin (Gemini Bio-Products, CA). Human M-CSF (Biolegend, CA) and soluble RANKL (PeproTech, NJ) were dissolved in alpha-MEM and stored at -80°C.

Bacteria sonication

AJ2 is a combination of 8 different strains of gram positive probiotic bacteria (*Streptococcus thermophiles, Bifidobacterium longum, Bifidobacterium breve, Bifidobacterium infantis, Lactobacillus acidophilus, Lactobacillus plantarum, Lactobacillus casei, and Lactobacillus bulgaricus*) used to induce differentiation of stem cells

(doi:10.3389/fimmu.2014.00269). AJ2 was weighed and resuspended in RPMI Medium 1640 containing 10% FBS at a concentration of 10mg per 1mL. The bacteria were thoroughly vortexed, then sonicated on ice for 15 seconds, at 6 to 8 amplitude. Sonicated samples were then incubated for 30 seconds on ice. After every five pulses, a sample was taken to observe under the microscope until at least 80 percent of cell walls were lysed. It was determined that approximated 20 rounds of sonication/incubation on ice, were conducted to achieve complete sonication. Finally, the sonicated samples (sAJ2) were aliquoted and stored in a -80 degrees Celsius freezer.

Purification of NK cells from the peripheral blood

Written informed consents, approved by UCLA Institutional Review Board (IRB), were obtained from healthy blood donors, and all procedures were approved by the UCLA-IRB. Peripheral blood was separated using Ficoll-Hypaque centrifugation, after which the white, cloudy layer, containing peripheral blood mononuclear cells (PBMC), was harvested, washed and re-suspended in RPMI 1640 (Invitrogen by Life Technologies, CA) supplemented with 10% FBS and plated on plastic tissue culture dishes. After 1-2 hours of incubation, non-adherent, human peripheral blood lymphocytes (PBL) were collected. NK cells were negatively selected and isolated from PBLs using the EasySep® Human NK cell enrichment kit purchased from Stem Cell Technologies (Vancouver, BC, Canada). Isolated NK cells were stained with anti-CD16 antibody, to measure NK cell purity using flow cytometric analysis. The isolated NK cell population was greater than 90% purity. Purified NK cells were cultured in RPMI Medium 1640 supplemented with 10% FBS (Gemini Bio-Products, CA), 1% antibiotic antimycotic, 1% sodium pyruvate, and 1% MEM non-essential amino acids (Invitrogen, Life Technologies, CA).

NK cell supernatants used for stem cell differentiation

As described above, human NK cells were purified from PBMCs of healthy donors. NK cells were left untreated, treated with sAJ2 at 1:3 (NK:sAJ2), and/or a combination of anti-CD16mAb (3μg/mL) and IL-2 (1,000 U/mL) for 18 hours before supernatants were removed and used for differentiation experiments. The amounts of IFN-γ produced by activated NK cells were assess with IFN-γ ELISA (Biolegend, CA, USA). OSCSCs were differentiated with gradual daily addition of increasing amounts of NK cell supernatants (of corresponding treatments). On average, to induce differentiation, a total of 4,500pg of IFN-γ containing supernatants, obtained from IL-2+anti-CD16mAb+sAJ2-treated NK cells, was added for 4 days to induce differentiation and resistance of OSCSCSs to NK cell-mediated cytotoxicity. Afterwards, target cells were washed with 1xPBS, detached and used for experiments.

Purification of monocytes from the peripheral blood

Written informed consents, approved by UCLA Institutional Review Board (IRB) were obtained from healthy blood donors, and all procedures were approved by the UCLA-IRB. Peripheral blood was separated using Ficoll-Hypaque centrifugation, after which the white, cloudy layer, containing peripheral blood mononuclear cells (PBMC), was harvested, washed and re-suspended in RPMI 1640 (Invitrogen by Life Technologies, CA) supplemented with 10% FBS and plated on plastic tissue culture dishes. After 1-2 hours of incubation, the adherent subpopulation of PBMCs was detached from the tissue culture plates. Monocytes were purified using the EasySep® Human monocyte cell enrichment kit obtained from Stem Cell Technologies (Vancouver, BC, Canada). Based on flow cytometric analysis of CD14 the antibody-stained, enriched monocyte cells, the monocyte population was found to have greater than a 95% purify.

Generation of osteoclasts

Osteoclasts were generated from PBMC-purified monocytes and cultured in alpha-MEM medium, containing M-CSF (25ng/mL) and RANK Ligand (RANKL) (25ng/mL), for 21 days. Medium was refreshed every 3 days with fresh alpha-MEM, containing M-CSF (25ng/mL) and RANKL (25ng/mL).

Analysis of human OSCSCs cell growth in immunodeficient and humanized mice

Animal research was performed under the written approval of the UCLA Animal Research Committee (ARC) in accordance to all federal, state, and local guidelines. Combined immunodeficient NOD.CB17-Prkdcscid/J and NOD.Cg-Prkdcscid Il2rgtm1Wjl/SzJ (NSG mice lacking T, B, and natural killer cells) were purchased from Jackson Laboratory and maintained in the animal facilities at UCLA in accordance with protocols approved by the UCLA animal research committee. Humanized-BLT (hu-BLT; human bone marrow/liver/thymus) mice were prepared on NSG background as previously described [71, 81].

Prior to tumor implantation, selected mice were fed $5x10^9$ AJ2 bacteria (the combination of 8 probiotic strains listed above) every other day for one week. This adjuvant therapy was continued every other day until the day of sacrifice. For each mouse, lyophilized AJ2 was resuspended in 200 μL of fat free milk, and fed to them via pipetting.

In vivo growth of human oral squamous carcinoma stem cells (OSCSCs) was determined by orthotopic cell implantation of tumor cells into hu-BLT mice. To establish orthotopic tumors, mice were first anesthetized using an isoflurane set up, and OSCSCs were then transferred by direct injection of $1x10^6$ cells mixed with 10 μl HC Matrigel (Corning, NY,USA) into the oral cavity, to the floor of the mouth. Immediately prior to tumor cells injection, 5.0-mg/kg carprofen

was injected subcutaneously, and this injection was repeated every 24 hours for 48 hours.

Following injection of tumor cells, all mice were continuously monitored for disease progression every other day. Mice were observed for overall signs of morbidity, such as loss of weight, ruffled fur, hunched posture, and immobility. Seven days after tumor implantation selected hu-BLT mice received $1.5x10^6$ human expanded NK cells via tail vein (IV) injection.

Cell dissociation and cell culture from tissues of tumor bearing hu-BLT and NSG mice

At the end of the experiment, mice were euthanized and oral tumor, liver, bone marrow, spleen and blood were obtained from hu-BLT or NSG mice. Single cell suspensions were obtained by digesting tissues using DMEM medium supplemented with collagenase II (1mg/mL) (oral tumor) (Invitrogen, CA) and DNAse (10u/mL) (Sigma-Aldrich, CA) and 1%BSA. The digested tissues were passed through 70 μM filters (Fisher Scientific, CA) to obtain single cell suspensions. Femurs and spleens were harvested from animals, and bone marrow cells and splenocytes were passed through 70 μM filters (Fisher Scientific, CA) to obtain single cell suspensions. Murine peripheral blood mononuclear cells (PBMCs) were obtained using Ficoll-Hypaque centrifugation of heparinized blood specimens. The white, cloudy layer, containing peripheral blood mononuclear cells (PBMCs), were harvested, washed and re-suspended in medium. Single cell suspensions of each tissue were cultured in the presence and/or absence of IL-2 (1000 units/mL) treatment, using RPMI 1640 media (Life Technologies, CA), supplemented with 10% FBS.

Purification of human T cells from hu-BLT mice

CD3+ T cells from hu-BLT mice were positively selected from splenocytes using

isolation kits from Stem Cell Technologies (Vancouver, BC, Canada). Cells were cultured at $1x10^6$ cells/mL in RMPI 1640 media (Life Technologies, CA), supplemented with 10% FBS, along with IL-2 (1000 units/mL) treatment. Flow-through cells (negative for CD3, following the positive selection for T cells) were also cultured in the same manner.

Surface staining

$1x10^5$ cells from each condition were stained in 100ul of cold 1%PBS-BSA with pre-determined optimal concentration of PE conjugated antibodies, as detailed in the experiments, and incubated at 4°C for 30 minutes. Then, cells were washed and resuspended in 1%PBS-BSA. The Epics C (Coulter) flow cytometer was used for cellular surface analysis.

^{51}Cr release cytotoxicity assay

^{51}Cr was purchased from Perkin Elmer (Santa Clara, CA). Standard ^{51}Cr release cytotoxicity assays were used to determine NK cell cytotoxic function in the experimental cultures and the sensitivity of target cells to NK cell mediated lysis. The effector cells ($1x10^5$ NK cells/well) were aliquoted into 96-well round-bottom microwell plates (Fisher Scientific, Pittsburgh, PA) and titrated at four to six serial dilutions. The target cells ($5x10^5$ OSCSCs) were labeled with 50μCi ^{51}Cr (Perkin Elmer, Santa Clara, CA) and chromated for 1 hour. Following incubation, target cells were washed twice to remove excess unbound ^{51}Cr. ^{51}Cr-labeled target cells were aliquoted into the 96-well round bottom microwell plates containing effector cells at a concentration of $1x10^4$ cells/well at a top effector:target (E:T) ratio of 5:1. Plates were centrifuged and incubated for a period of 4 hours. After a 4-hour incubation period, the supernatants were harvested from each sample and counted for released radioactivity using the

gamma counter. Total (containing ^{51}Cr-labeled target cells) and spontaneous (supernatants of target cells alone) release values were measured and used to calculate the percentage specific cytotoxicity. The percentage specific cytotoxicity was calculated using the following formula:

$$\% \text{ Cytotoxicity} = \frac{\text{Experimental cpm - spontaneous cpm}}{\text{Total cpm – spontaneous cpm}}$$

LU $30/10^6$ is calculated by using the inverse of the number of effector cells needed to lyse 30% of target cells x100.

Enzyme-Linked Immunosorbent Assays (ELISAs) and multiplex cytokine assay

Human ELISA kits for IFN-γ and IL-10 were purchased from Biolegend (San Diego, CA). ELISA was performed to detect the level of IFN-γ and IL-10 produced from cell cultures. The assay was conducted as described in the manufacturer's protocol. Briefly, 96-well EIA/RIA plates were coated with diluted capture antibody corresponding to target cytokine and incubated overnight at 4°C. After 16-18 hours of incubation, the plates were washed 4 times with wash buffer (0.05% Tween in 1xPBS) and blocked with assay diluent (1%BSA in 1xPBS). The plates were incubated for 1 hour at room temperature, on a plate shaker at 200rpm; plates were washed 4 times following incubation. Then, 100uL of standards and samples collected from each culture were added to the wells and incubated for 2 hours at room temperature, on the plate shaker at 200rpm. After incubation, plates were washed 4 times, loaded with detection antibody, and incubated for 1 hour at room temperature, on the plate shaker at 200rpm. After 1 hour of incubation, the plates were washed 4 times; wells were loaded with Avidin-HRP solution and incubated for 30 minutes at room temperature, on the plate shaker at 200rpm. After washing the plates 5 times with wash buffer; 100uL of TMB substrate solution was added to the wells and

plates were incubated in the dark until they developed a desired blue color (or up to 30 minutes). Then, 100uL of stop solution (2N H_2SO_4) was added per well to stop the reaction. Finally, plates were read in a microplate reader, at 450nm to obtain absorbance values (Biolegend, ELISA manual).

The levels of cytokines and chemokines were examined by multiplex assay, which was conducted as described in the manufacturer's protocol for each specified kit. Analysis was performed using a Luminex multiplex instrument (MAGPIX, Millipore, Billerica, MA) and data was analyzed using the proprietary software (xPONENT 4.2, Millipore, Billerica, MA).

Statistical analysis

An unpaired, two-tailed student t-test was performed for the statistical analysis of two groups. One-way ANOVA with a Bonferroni post-test was used to compare more than two groups.

CHAPTER 1

Specific Aim 1: **To investigate the role of probiotics in the activation of NK cells.**

RESULTS

Probiotic bacteria induce cytokine secretion but have no effect on cytotoxicity.

To investigate the effect of probiotics on NK cell function, NK cells were cultured either with or without sAJ2 under different activation conditions. NK cells, left as control or activated with IL-2 or IL-2+anti-CD16mAb, treated with sAJ2 probiotic induced higher levels of IFN-γ and IL-10 **(Fig. 1)**. Although activated NK cells secreted IFN-γ, treatment of activated NK cells with sAJ2 bacteria significantly increased the levels of IFN-γ **(Fig. 1A)**. Treatment with sAJ2 induced secretion of IL-10 in all NK conditions, especially for control NK cells (not activated) **(Fig. 1B)**.

To understand the effect of sAJ2 on NK cytotoxic function, ^{51}Cr release assay was conducted with NK cells treated with or without bacteria. Although sAJ2 bacteria induced cytokine secretion function in NK cells, they had no effect on their cytotoxic function **(Fig. 2)**. NK cells, untreated as well as activated, exhibited no significant change in their ability to target and lyse OSCSCs when treated with either live or sonicated AJ2 bacteria **(Fig. 2)**. Thus, sAJ2 bacteria enhance the functional effect of NK cells through cytokine secretion, while NK cells also maintain the same level of cytotoxicity.

Supernatants of sAJ2 bacteria treated, split anergized NK cells induce differentiation and resistance of OSCSCs to NK cell-mediated cytotoxicity.

To investigate the differentiation capability of split anergized NK cells (NK cells activated with anti-CD16mAb and IL-2) treated with sAJ2, NK cells were activated and treated as described in Figure 3, and supernatants were collected and used to treat stem-like tumor cells, OSCSCs, as described in the Materials and Methods section. Following differentiation, surface expression of key cell surface markers was studied. MHC-I, CD54 and B7H1 were found to be upregulated on the surface of OSCSCs differentiated with supernatants from split anergized NK cells, both alone and in combination with sAJ2, although treatment with sAJ2 in combination significantly increased their levels of expression **(Fig. 3)**. There was also a moderate decrease in the expression of CD44 stem cell marker for OSCSCs differentiated with split anergized NK supernatants, both alone and in combination with sAJ2. Supernatants from NK cells treated with sAJ2 alone were not effective in differentiating OSCSCs **(Fig. 3)**.

Also, following differentiation with supernatants, the various conditions of OSCSCs were assayed for their susceptibility to NK cell-mediated lysis using ^{51}Cr release assay **(Fig. 4)**. OSCSCs treated with supernatants obtained from untreated or sAJ2 alone treated NK cells showed no change in their susceptibility to NK cell-mediated lysis. On the other hand, treatment of OSCSCs with supernatants from NK cells treated with IL-2+anti-CD16mAb resulted in tumor resistance to NK cell-mediated lysis. OSCSCs showed significantly more resistance to IL-2 activated NK cell-mediated lysis following treatment with supernatants from IL-2+anti-CD16mAb+sAJ2 activated NK cells compared to the controls, including the split anergized control ($P < 0.05$) **(Fig. 4)**.

Differentiation induced by split anergized NK cells is significantly mediated via cytokine secretion of IFN-γ and TNF-α

To understand the mechanism through which OSCSCs differentiate and become resistant to NK cell-mediated lysis, OSCSCs were treated with supernatants obtained from NK cells treated with IL-2+anti-CD16mAB+sAJ2, as well as antibodies against IFN-γ and/or TNF-α. As described earlier, supernatants from NK cells treated with IL-2+anti-CD16mAb+sAJ2 induced differentiation and resistance of tumors to NK cell-mediated cytotoxicity **(Fig. 3-6)**. Anti-IFN-γ treatment alone prevented the surface expression modulation of CD54, MHC-I and B7H1 on differentiated OSCSCs, while anti-TNF-α only prevented CD54 surface expression upregulation. Meanwhile, OSCSCs supplemented with supernatants from NK cells treated with IL-2+anti-CD16mAb+sAJ2 with the combination of anti-IFN-γ and anti-TNF-α showed inhibition of surface expression modulation to the supplementation **(Fig. 5)**.

When either anti-TNF-α or anti-IFN-γ were added to supernatant-treated cells, there was either no or a moderate inhibitory effect on the resistance of OSCSCs to NK cell-mediate lysis **(Fig. 6)**. On the other hand, when both antibodies were used together, OSCSCs maintained their sensitivity to NK cell-mediated lysis **(Fig. 6)**. Additionally, differentiation of OSCSCs with IL-2+anti-CD16mAb+sAJ2 activated NK cell supernatants resulted in tumor growth inhibition, in comparison to untreated or split anergized NK supernatant treated OSCSCs **(Fig. 7)**. When a combination of anti-IFN-γ and anti-TNF-α were used along with the supernatants from IL-2+anti-CD16mAb+sAJ2 activated NK cells, tumor growth was restored to levels seen in untreated OSCSCs **(Fig. 7)**.

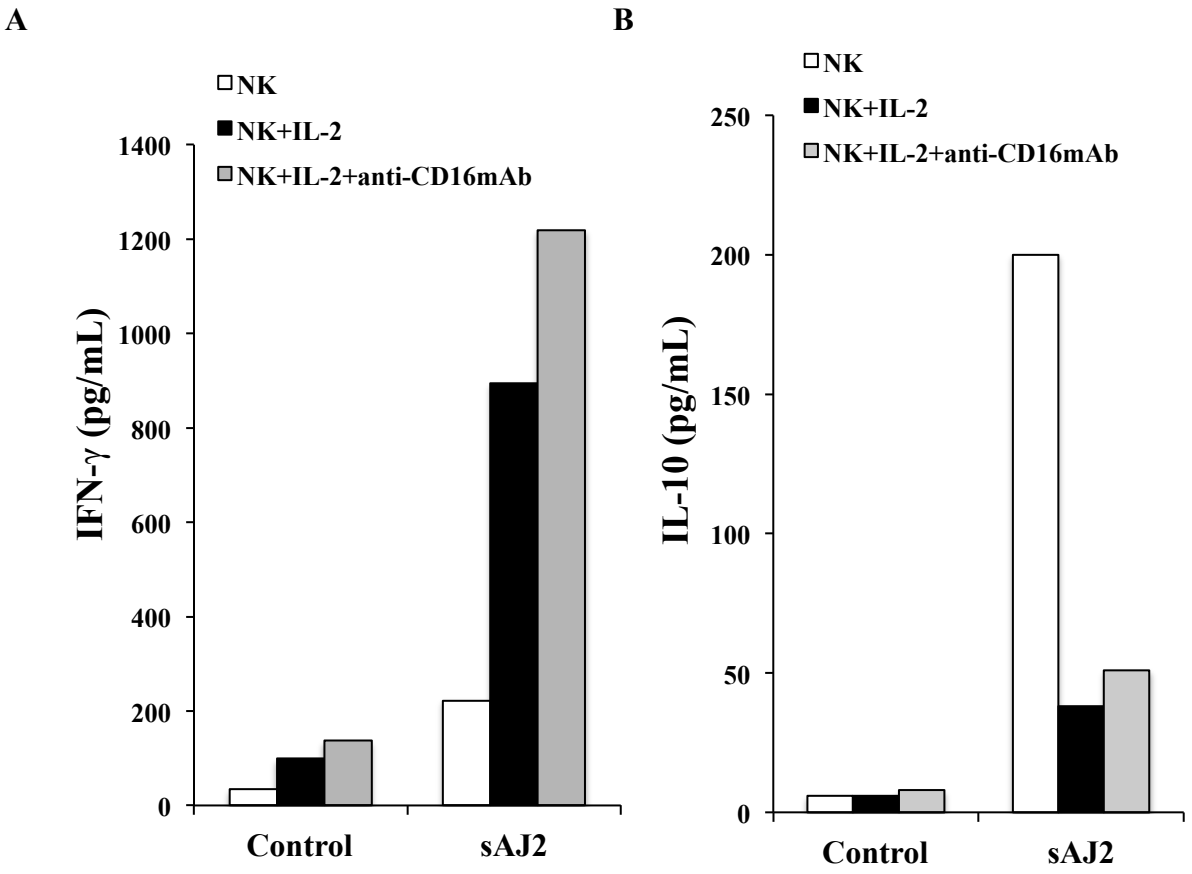

Figure 1. Treatment of NK cells with probiotic bacteria induces higher secretion of IFN-γ and anti-inflammatory cytokine, IL-10.

Purified NK cells ($1x10^6$/mL) were left untreated, treated with IL-2 (1000 units/mL), or anti-CD16mAb (3 μg/mL) and IL-2 (1000 units/mL), with or without probiotic bacteria, sAJ2, at a 1:5 (NK cell:bacteria) ratio, for 18 hours. Supernatants of cultures were harvested and used for multiplex array analysis. Above are the levels of secretion for IFN-γ **(A)** and IL-10 **(B)**.

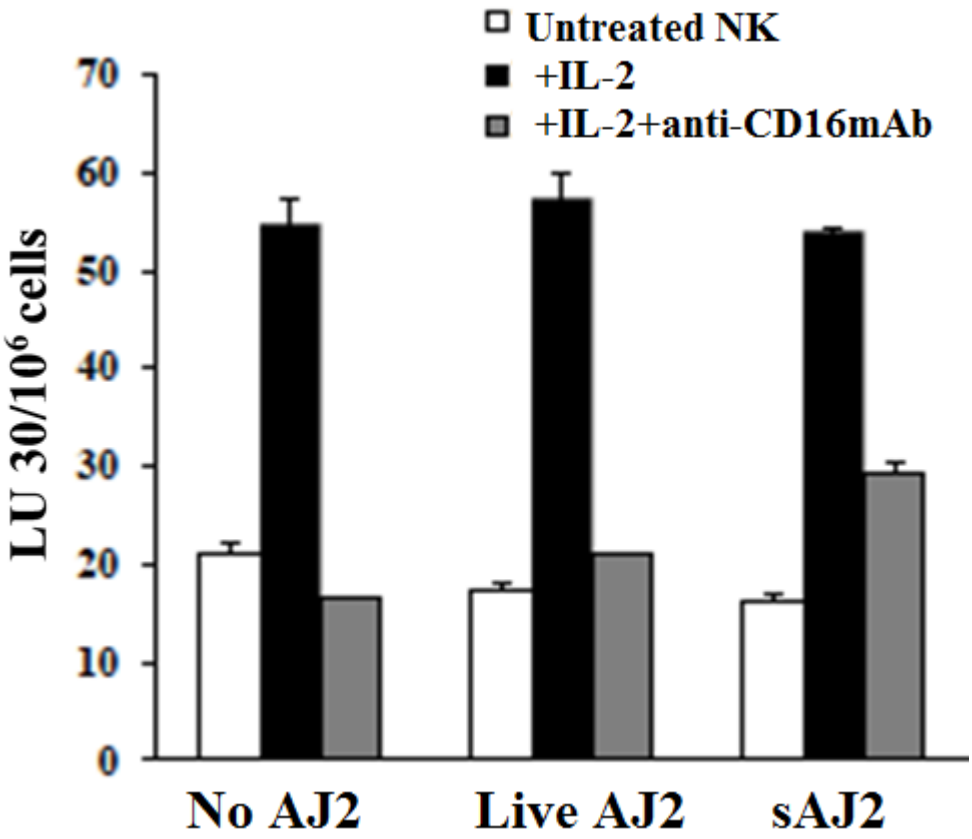

Figure 2. Probiotic bacteria do not affect NK cell-mediated cytotoxicity against OSCSCs.

Purified NK cells ($1x10^6$/mL) were left untreated, IL-2 (1000 units/mL) treated, or anti CD16mAb (3 µg/mL) and IL-2 (1000 units/mL) treated, and cultured in the presence or absence of live or sonicated AJ2 at a 1:3 (NK cell:bacteria) ratio, for 12-18 hours. Following overnight incubation, they were added to ^{51}Cr labeled OSCSC cells (target cells). NK cell cytotoxicity was determined by conducting a standard 4-hour ^{51}Cr release assay. A gamma counter was used to measure the radioactivity released into the supernatants. Levels of NK cell-mediated cytotoxicity against radioactively labeled OSCSCs were determined using lytic units (LU $30/10^6$).

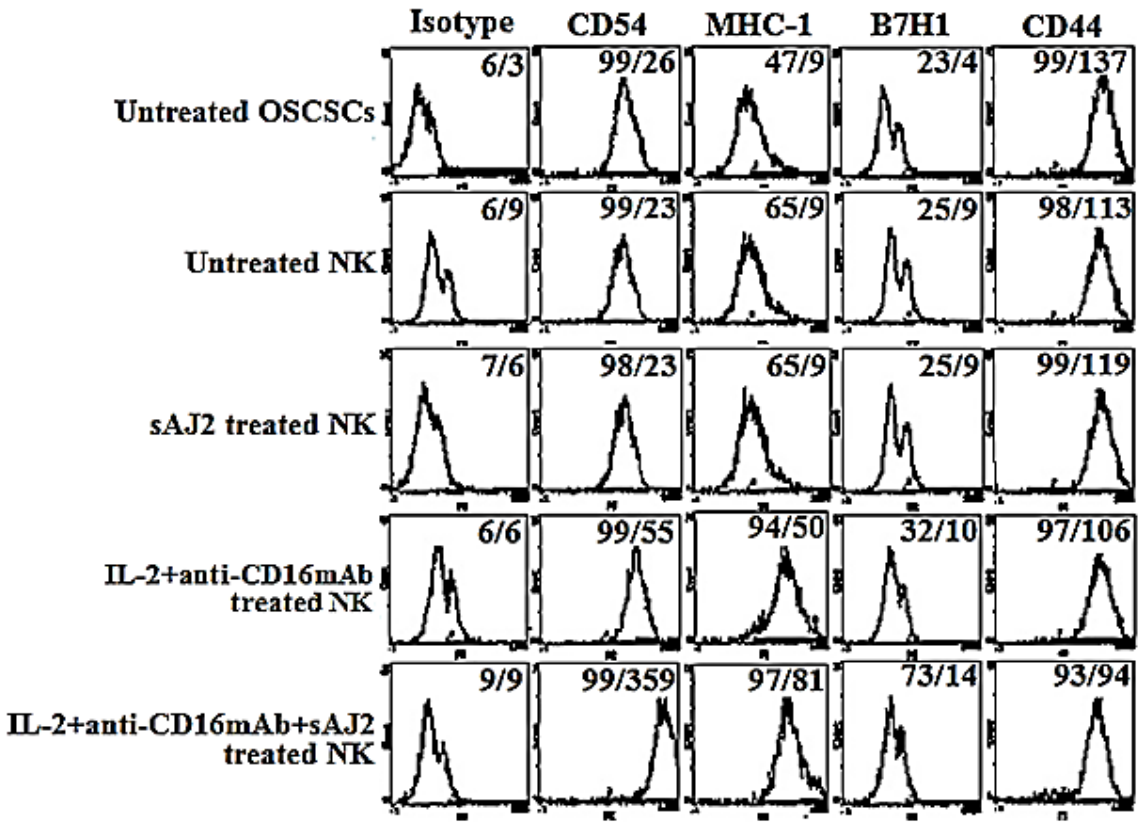

Figure 3. Surface expression trend demonstrates upregulation of differentiation markers in OSCSCs differentiated with IL-2+anti-CD16mAb+sAJ2 activated NK cells.

Purified NK cells were left untreated or treated with anti-CD16mAb (3µg/mL) and IL-2 (1000 units/mL), with or without sonicated AJ2 (sAJ2) at a 1:3 (NK cell:bacteria) ratio, for 18 hours. Afterwards, the supernatants from each NK sample were harvested and used to treat/differentiate OSCSCs for 4 days. OSCSCs were detached from the tissue culture plates and $5x10^4$ cells from each treatment were used to measure surface expression of surface markers via flow cytometry. PE conjugated antibodies against isotype control, CD54, MHC-I, B7H1 and CD44 were used to stain untreated OSCSCs or those treated with NK cell supernatants, as detailed in the figure. Isotype control antibodies were used as controls. The numbers on the right hand corner are the percentages and the mean channel fluorescence intensities for each histogram.

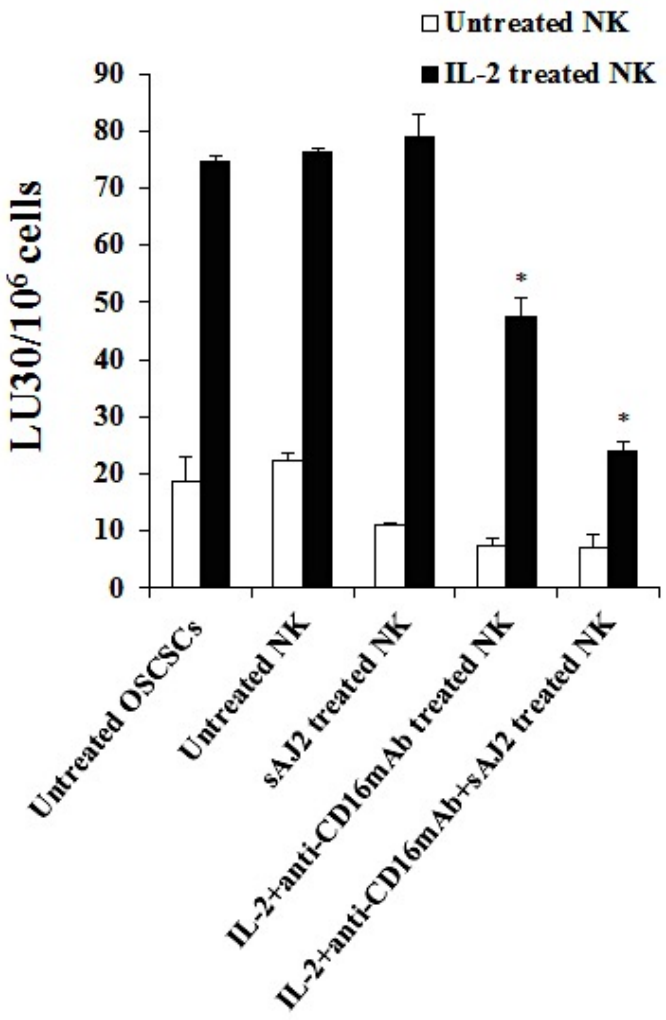

Figure 4. OSCSCs treated with supernatants of split anergized NK cells were significantly more resistant to NK cell-mediated cytotoxicity—highest level of resistance in those treated with supernatants of split anergized NK cells in combination with sAJ2.

Purified NK cells were treated as described in Figure 3. Afterwards, the supernatants from each NK sample were harvested and used to treat/differentiate OSCSCs for 4 days. OSCSCs were detached from the tissue culture plates and their sensitivity to NK cell-mediated lysis was evaluated using a standard 4-hour ^{51}Cr release assay. Levels of NK cell-mediated cytotoxicity against radioactively labeled OSCSCs conditions were determined using lytic units (LU $30/10^6$).

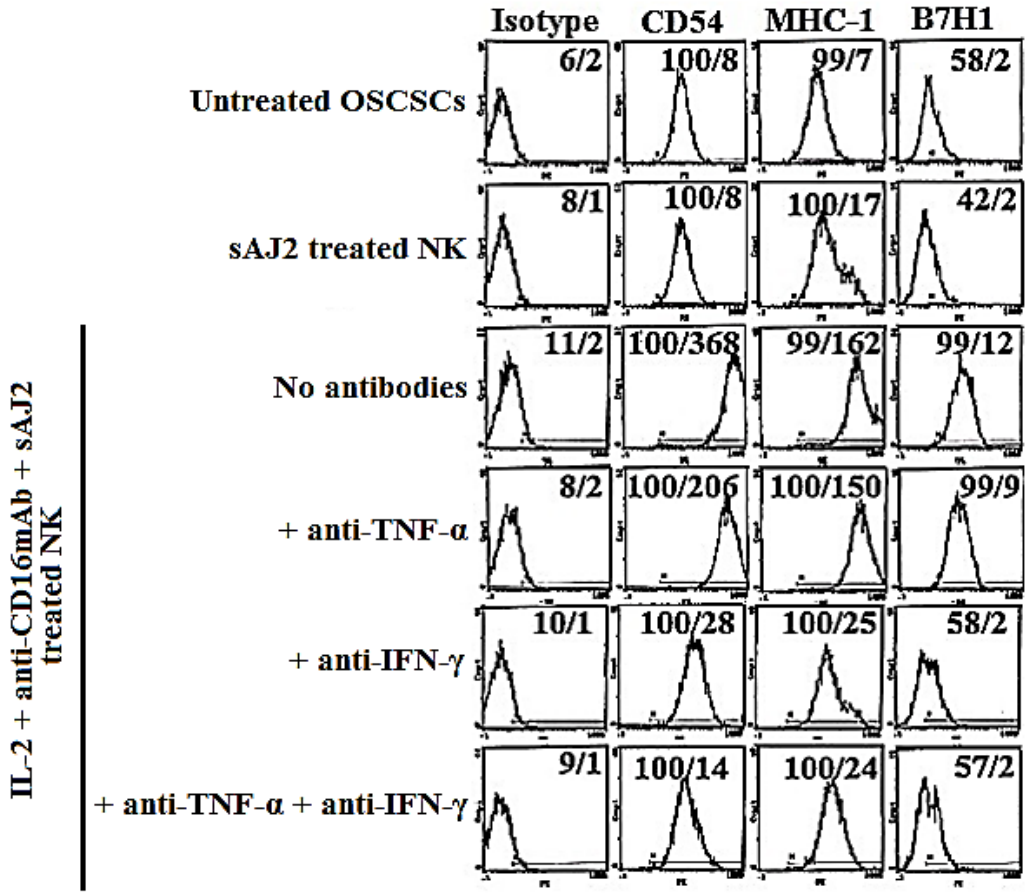

Figure 5. Induction of differentiation of OSCSCs treated with IL-2+anti-CD16mAb+sAJ2 NK cell supernatant is mediated by the combination of IFN-γ and TNF-α secreted by NK cells.

Purified NK cells ($1x10^6$/mL) were treated with sAJ2 alone at a 1:3 (NK cell:bacteria) ratio, or in combination with IL-2 (1000 units/mL) and anti-CD16mAb (3μg/mL), for 18 hours. Afterwards, the supernatants from each NK sample were harvested and used to treat/differentiate OSCSCs for 4 days. Anti-IFN-γ (1:100) and anti-TNF-α (1:100) antibodies were added to OSCSCs before the start of NK sup treatments. OSCSCs were detached from the tissue culture plates, and $5x10^4$ cells from each treatment were used to measure surface expression of surface markers via flow cytometry. PE conjugated antibodies against isotype control, CD54, MHC-I, and B7H1 were used to stain untreated OSCSCs or those treated with NK cell supernatants (with or without antibodies against IFN-γ and/or anti-TNF-α), as detailed in the figure. Isotype control antibodies were used as controls. The numbers on the right hand corner are the percentages and the mean channel fluorescence intensities for each histogram.

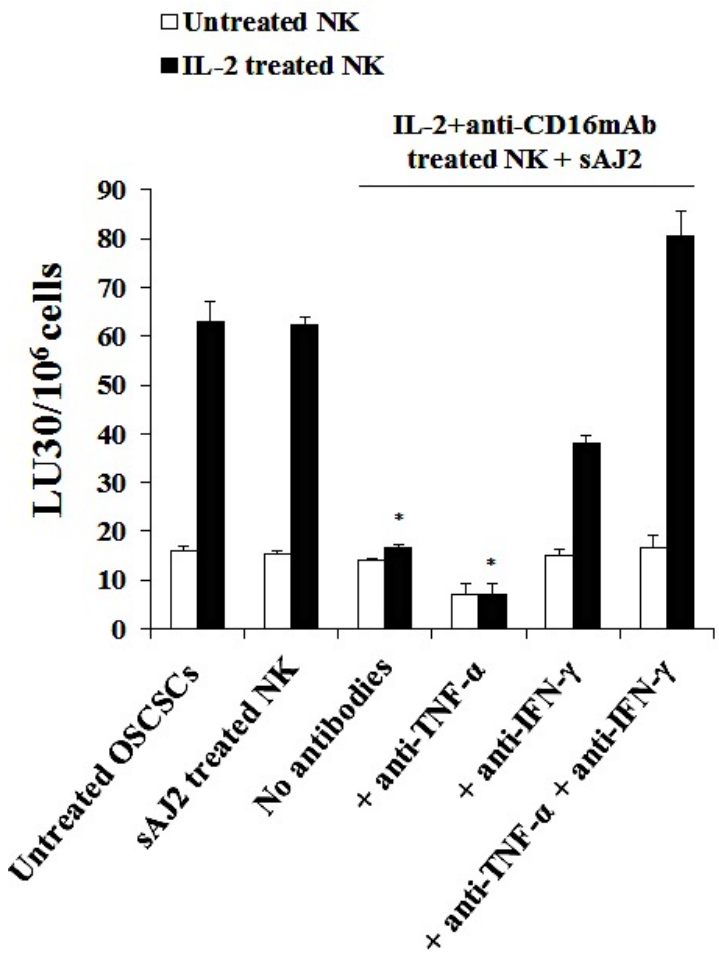

Figure 6. Induction of differentiation, and therefore, resistance to NK cell mediated lysis of OSCSCs treated with IL-2+anti-CD16mAb+sAJ2 NK cell supernatant is mediated by the combination of IFN-γ and TNF-α secreted by NK cells.

Purified NK cells were treated as described in Figure 5. Afterwards, supernatants from each NK sample were harvested and used to treat/differentiate OSCSCs for 4 days. Anti-IFN-γ (1:100) and anti-TNF-α (1:100) antibodies were added to OSCSCs before the start of NK sup treatments. OSCSCs were then detached from the tissue culture plates and their sensitivity to NK cell-mediated lysis was evaluated using a standard 4-hour ^{51}Cr release assay. Levels of NK cell-mediated cytotoxicity against radioactively labeled OSCSCs conditions were determined using lytic units (LU 30/10^6).

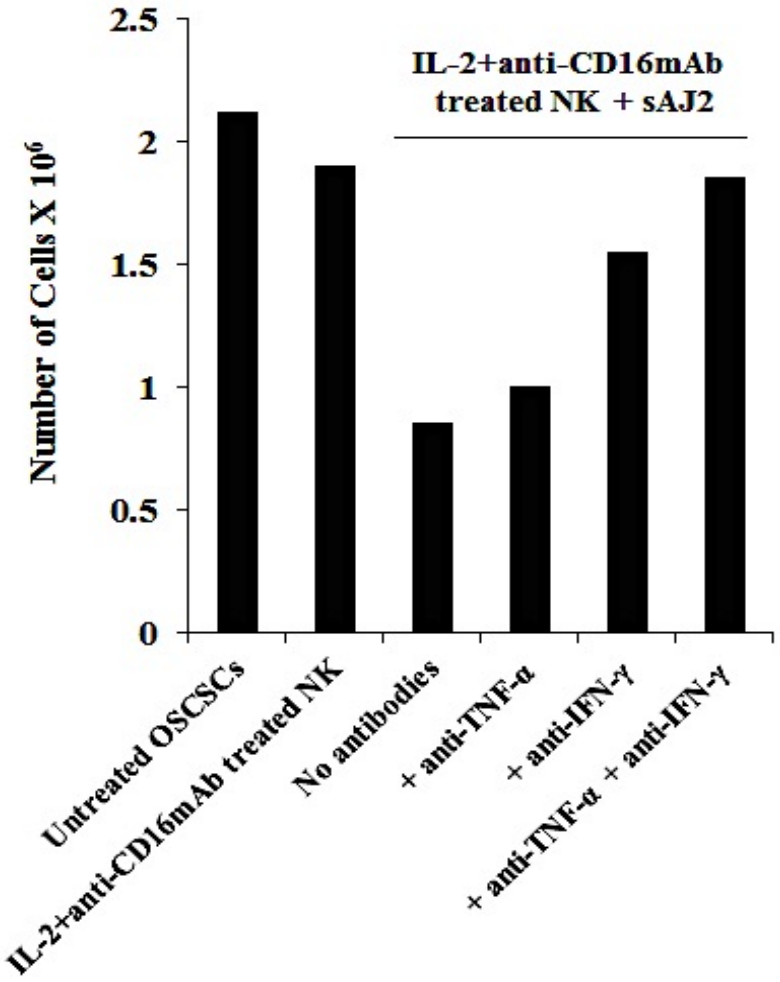

Figure 7. Induction of differentiation, also resulting in growth inhibition of OSCSCs treated with IL-2+anti-CD16mAb+sAJ2 NK cell supernatant, is mediated by the combination of IFN-γ and TNF-α secreted by NK cells.

Purified NK cells were treated as described in Figure 5. Afterwards, supernatants from each NK sample were harvested and used to treat/differentiate OSCSCs for 4 days. Anti-IFN-γ (1:100) and anti-TNF-α (1:100) antibodies were added to OSCSCs before the start of NK sup treatments. OSCSCs were then detached from the tissue culture plates and cells were counted via microscopy.

CHAPTER 2

Specific Aim 2: **To investigate the capability of osteoclasts in expanding NK cells in combination with probiotic bacteria.**

RESULTS

sAJ2 in combination with osteoclasts expand NK cells, and not T cells, maintaining them for a longer period of time

NK cells were isolated from healthy donor PBMCs, and NK purity was determined using CD3 and CD16/CD56 antibodies before cultures were conducted. NK cells were then activated with anti-CD16mAb and IL-2 18-20 hours before co-culturing them with sAJ2 alone ("Control") or sAJ2 in combination with osteoclasts ("+Osteoclasts") **(Fig. 8)**. NK cells treated with sAJ2 failed to expand and maintain NK cell purity over time, whereas NK cells cultured with sAJ2 and osteoclasts maintained NK purity and expansion for a long period of time. The combination of osteoclasts and sAJ2 preferentially expanded NK cells while maintaining a low proportion of T cells throughout the cultures **(Fig. 8)**.

Expanded NK cells are highly functional, both in terms of cytotoxicity and cytokine secretion functions

To investigate the functional ability of sAJ2 and osteoclast-expanded NK cells, cell mediated cytotoxicity and IFN-γ secretion levels were measured. NK cells activated with anti-CD16mAb and IL-2, as described previously, co-cultured with sAJ2 and osteoclasts lysed significantly more OSCSCs than NK cells co-cultured with sAJ2 alone; and there was a significant increase in cytotoxicity of expanded NK cells from day 9 to day 15 **(Fig. 9)**,

correlating with higher expansion of NK cells in co-culture with sAJ2 and osteoclasts after day 14 **(Fig. 11)**. IL-2 and anti-CD16mAb activated NK cells cultured with sAJ2 and osteoclasts secreted significantly higher amounts of IFN-g, compared to NK cells activated with IL-2 and anti-CD16mAb, co-cultured with sAJ2 alone **(Fig. 10)**.

sAJ2 in combination with osteoclasts maintain a high level of NK expansion for an extended time period

To investigate the expansion rate of expanded NK cells (activated with anti-CD16mAb and IL-2 overnight, and co-cultured with sAJ2 and osteoclasts), cells were counted via microscopy, and at various time points **(Fig. 11)**. Upon analysis of NK cell expansion rate and population doubling (defined by the log of the ratio of the final count to the baseline count divided by the log of 2) it was found that NK cells expanded 21,000-132,000 fold at day 20 and 0.3-5.1 million fold on day 31, with 17-21 population doublings within 4 weeks **(Table 1)**.

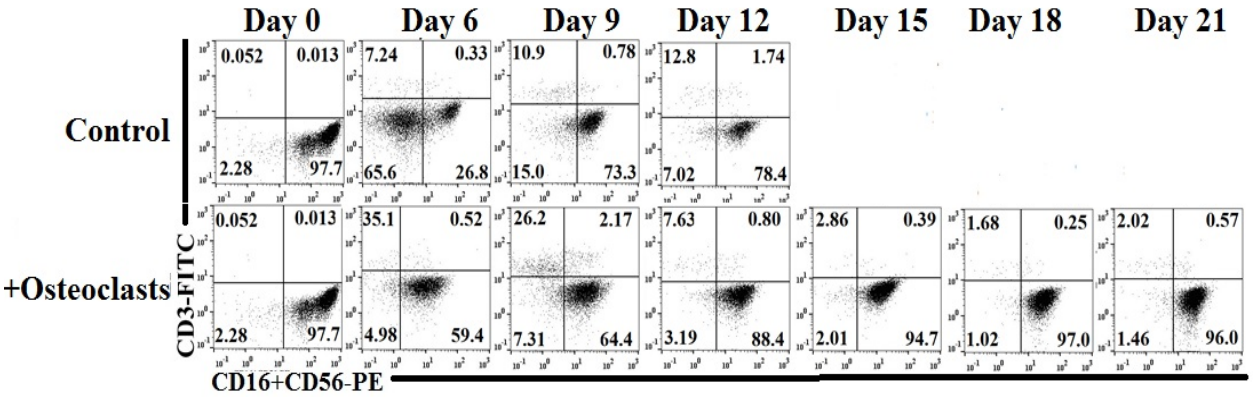

Figure 8. sAJ2 in combination with osteoclasts expand NK cells, and not T cells, maintaining them for a longer period of time.

Purified NK cells and monocytes were obtained from PBMCs of healthy donors, as described in the Materials and Methods section. To generate osteoclasts, monocytes were cultured in alpha-MEM media containing M-CSF (25 ng/mL) and RANKL (25 ng/mL), for 21 days, replenishing media every 3 days. Then purified NK cells ($1x10^6$ cells/mL) were treated with the combination of IL-2 (1000 units/mL) and anti-CD16mAb (3 µg/mL) for 18 hours before they were co-cultured with sAJ2, with or without autologous osteoclasts at a 1:2:4 (OC:NK:sAJ2) ratio. Culture medium of expanding NK cells was refreshed and re-supplemented with IL-2 (1000 units/mL) at respective days detailed in the figure. Surface expression levels of CD3, CD16, and CD56 were analyzed on respective days, using flow cytometry.

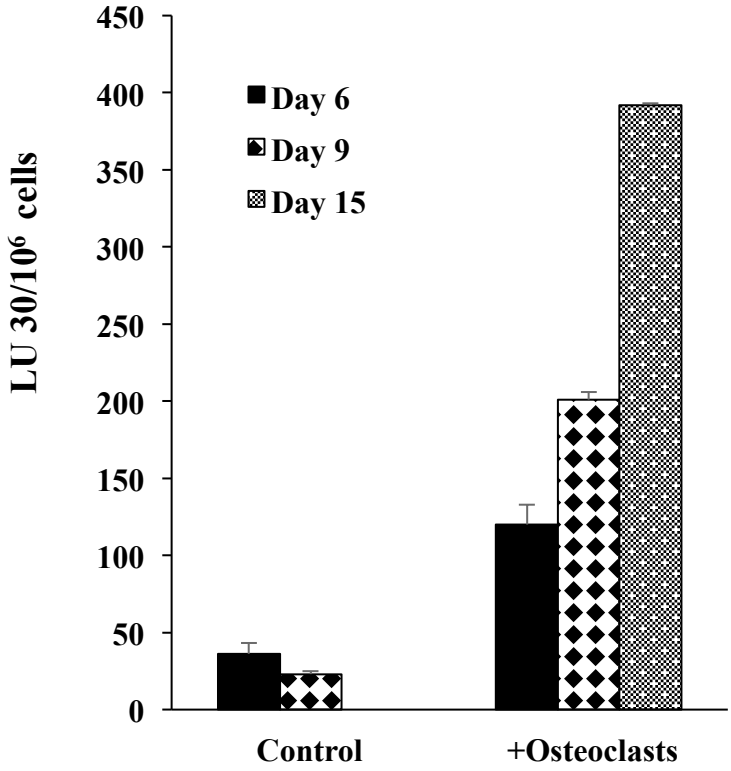

Figure 9. NK cells expanded with osteoclasts as feeder cells are highly cytotoxic for an extended length of time.

Purified NK cells and monocytes from PBMCs were cultured and treated as described in Figure 8. At days 6, 9 and 15, NK cell-mediated cytotoxic function of these expanded NK cells were measured using a standard 4-hour ^{51}Cr release assay. Levels of NK cell-mediated cytotoxicity of these NK cell conditions, against radioactively labeled OSCSCs (target cells) were determined using lytic units (LU $30/10^6$).

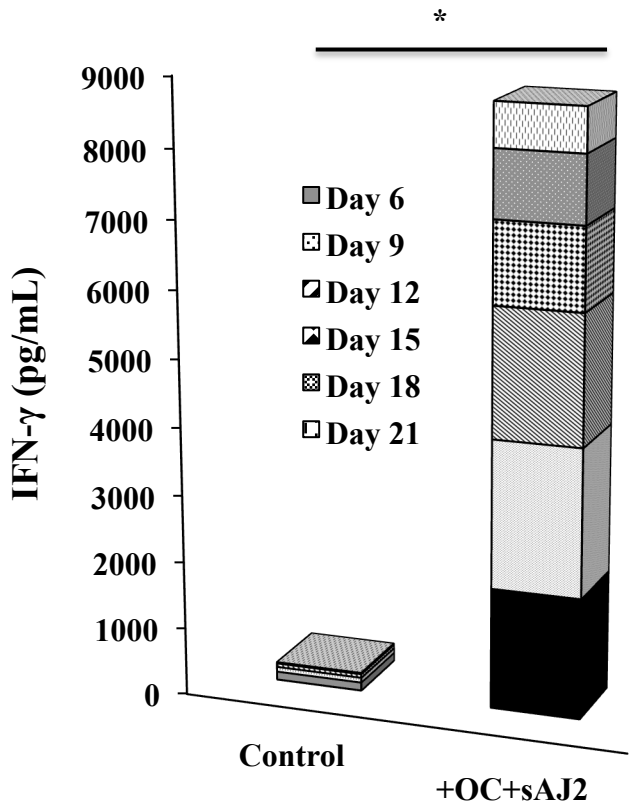

Figure 10. Osteoclast-expanded NK cells secrete significantly higher levels of cytokines for an extended period of time.

Purified NK cells and monocytes from PBMCs were cultured and treated as described in Figure 8. Purified NK cells ($1x10^6$ cells/mL) were treated with the combination of IL-2 (1000 units/mL) and anti-CD16mAb (3 μg/mL) for 18 hours before they were co-cultured with sAJ2, with or without autologous osteoclasts at a 1:2:4 (OC:NK:sAJ2) ratio. On days 6, 9, 12, 15, 18, and 21, supernatants of expanding NK cells were harvested and levels of IFN-γ were measured using human IFN-γ ELISA. Cells were replenished with fresh culture medium and re-supplemented with IL-2 (1000 units/mL) at respective days detailed in the figure.

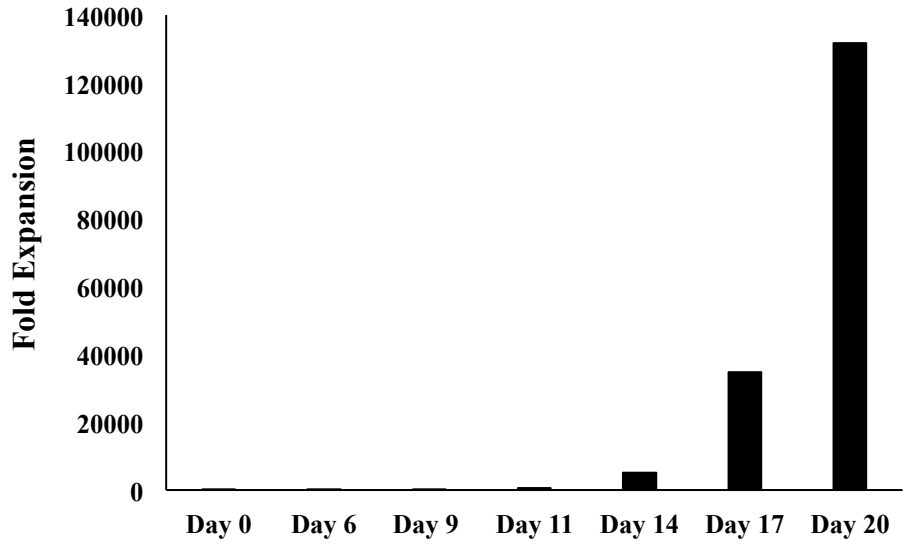

Figure 11. Fold expansion of osteoclast-expanded NK cells.

Highly purified NK cells and monocytes were obtained from PBMCs of healthy donors. To generate osteoclasts, monocytes were cultured in alpha-MEM media containing M-CSF (25 ng/mL) and RANKL (25 ng/mL) for 21 days. For expansion, purified NK cells ($1x10^6$ cells/mL) were treated with the combination of IL-2 (1000 units/mL) and anti-CD16mAb (3 µg/mL) for 18 hours; then they were co-cultured with autologous osteoclasts in the presence of sAJ2 at a 1:2:4 (OC:NK:sAJ2) ratio. Culture medium of expanding NK cells was refreshed and re-supplemented with IL-2 (1000 units/mL) at respective days detailed in the figure. Fold expansion was determined based on manual cell counts, via microscopy.

NK Source	Feeder cells	Expansion	References
Negative selection for NKs from PBMCs	Autologous and allogeneic osteoclasts	**21,000-132,000 fold** expansion at 20 days, 0.3-5.1 million at 31 days; **17-21 population doublings** (avg. 19) at 4 weeks	Dr. Jewett lab, *manuscript in prep*
Whole PBMCs or purified NKs	Irradiated PBMCs, Wilms tumor cell line, K562-mb15-41BBL, irradiated EBV-TM-LCL, or none	**4-5,712 fold** at 14-21 days	[52, 55, 82-88]
Whole PBMCs used initially, residual T-cells removed after 7 days (anti-CD3 Dynabeads), genetically modified with TERT for immortalization	K562-mb15-41BBL (continued stimulation)	TERT transformed: (**130-227 population doublings** over 1000 days) Non-transformed: (**11-20 population doublings** at 8-15 weeks)	[89]
Cord Blood (CB), CD34+ selection	None	**2,000-15,000 fold** at 5 weeks	[90, 91]
NK-92 (cell line)	None	**218- 250 fold** at 15-17 days	[92]

Table 1. NK expansion methodologies.

This table summarizes methods detailed in primary articles describing various NK expansion protocols, including source of NK cells, feeder cells used (if applicable), as well as the expansion success obtained (including the number of days required to achieve such expansion).

CHAPTER 3

Specific Aim 3: To investigate the use of adjuvant probiotic supplementation in combination with osteoclast-expanded NK immunotherapy in hu-BLT mice.

RESULTS

The hu-BLT mouse model was used to investigate the use of adjuvant probiotic supplementation in combination with NK cell-based adoptive immunotherapy using the expansion method described in Specific Aim 2 (detailed in the Materials and Methods section), to target cancer stem-like cells. **Figure 12** provides a detailed description of the experimental design.

NK immunotherapy resulted in the recruitment of T cells in various tissue compartments; AJ2 probiotic supplementation further increased this effect

To investigate the immunomodulatory effect of NK immunotherapy in the humanized mouse cancer model, multiple tissue compartments were harvested and analyzed for immune cell markers. In all immune tissue compartments harvested from the mice on the day of sacrifice, including bone marrow **(Table 2A)**, blood **(Table 3)** and spleen **(Table 5A)**, CD3+ immune cells (T cells) had an elevated presence in mice that received NK immunotherapy—the combination with AJ2 supplementation demonstrated a higher level of T cell presence. The presence of higher T cells was observed during later time points of cultures, as well **(Tables 2B, 5B)**. Bone marrow harvested from mice also showed an elevated presence of MDSCs (myeloid derived suppressor cells) in mice that received NK immunotherapy **(Table 12)**.

In addition to immune tissue showing elevated levels of T cells, this trend was also observed in the immune cells (CD45+ cells) present within the tumors resected from the animals **(Table 8)**. Mice that received NK immunotherapy showed a higher percentage of T cells within the immune population present in the tumors, with AJ2 supplementation showing a slightly higher level. The condition of AJ2 supplementation alone as treatment showed a much higher level of CD3 cell infiltration as compared to the control receiving only oral tumor injection **(Table 8)**.

NK immunotherapy treatment increased the cytokine secretion levels in various tissue compartments, while AJ2 probiotic supplementation further increased cytokine levels

To understand the effect of NK immunotherapy and probiotic supplementation on cytokine levels within various tissue compartments, tissues were harvested and analyzed for cytokine secretion levels. NK immunotherapy, both alone and in combination with AJ2 supplementation induced a high level of IFN-γ secretion during various time points of culture in PBMCs **(Fig. 16),** splenocytes **(Fig. 18, Table 6)**, and CD3 depleted splenocytes **(Fig. 22)**. Levels of IFN-γ were much higher in the NK immunotherapy in combination with AJ2 supplementation, for various culture time points from bone marrow cells **(Fig. 13)**, splenocytes **(Fig. 18, Table 6)** and CD3 cells isolated from splenocytes **(Fig. 20)**. Sera collected from mice immediately following sacrifice showed elevated levels of IFN-γ in mice receiving NK immunotherapy—much higher levels in the combination of NK immunotherapy with AJ2 supplementation **(Table 4)**.

Mice receiving NK immunotherapy and/or AJ2 supplementation showed increased levels of IL-10 cytokine in the sera **(Table 4A)**, while only NK immunotherapy receiving mice showed

elevated levels of IL-10 in cell cultures conducted using bone marrow cells **(Fig. 14B)**, splenocytes **(Fig. 19)**, CD3 cells isolated from splenocytes **(Fig. 21)**, and CD3 depleted splenocytes **(Fig. 23)**. Probiotic supplementation along with NK immunotherapy synergistically increased the level of IL-10 secreted by bone marrow cells **(Fig. 14)**, splenocytes **(Fig. 19)**, and CD3 cells isolated from splenocytes **(Fig. 21)**, observed at various time points.

Other cytokines that followed a similar trend include the elevation of IL-23 and IL-17 in the sera of mice receiving NK immunotherapy, with a significant increase in IL-23 levels in the NK immunotherapy combined with AJ2 supplementation **(Table 4A)**. Certain markers, such as IL-8, MIP-3α and ITAC were much higher in the tumor only control group, indicating a potential immunological marker for oral cancer **(Table 4B)**.

Tumor-bearing mice had reduced cytotoxic function in various tissue compartments, while mice receiving NK immunotherapy treatment had significantly improved cytotoxic functions

To investigate the cytotoxic function of NK cells within these tissue compartments, ^{51}Cr release assay was conducted using immune cells from harvested tissues. PBMCs were cultured as described in Figure 15, and on day 7, they were used in ^{51}Cr release assay to measure their cytotoxic function. PBMCs from healthy control (received only AJ2 supplementation and no tumor) were highly cytotoxic, and mice receiving NK immunotherapy also had a high level of cytotoxicity. The tumor control group should very low cytotoxicity, even compared to the group receiving AJ2 supplementation as a control treatment for the tumor **(Fig. 15)**. Splenocytes cultured as described in Figure 17, were also used in ^{51}Cr release assay to measure their cytotoxic function. Only splenocytes of the tumor control group had a significantly reduced level

of cytotoxicity compared to the other groups **(Fig. 17)**. Cytotoxic levels of NK immunotherapy and/or AJ2 supplementation groups were either comparable to or higher than the control (no tumor bearing) group **(Fig. 17)**.

NK immunotherapy, both alone and in combination with AJ2 supplementation, prevented tumor growth *in vivo*

Following sacrifice of animals, oral tumors were resected from the hu-BLT mice. When comparing sizes side-by-side, it was visibly clear that mice receiving NK immunotherapy had smaller tumors **(Fig. 24)**. This information was further validated through both measurements of the tumors on a scale, as well as tumor cell counts following dissociation of the harvested tumors **(Table 7)**. Tumors of mice receiving NK immunotherapy weighted less and were composed of less tumor cells compared to the other controls.

Tumors dissected from mice receiving NK immunotherapy were more differentiated, resistant to NK cell-mediated cytotoxicity, and slower growing

To investigate the effectiveness of NK immunotherapy in differentiating OSCSCs *in vivo*, hu-BLT mice were treated as described in Figure 12. Following sacrifice, resected tumors were analyzed using flow cytometry. Mice receiving NK immunotherapy following oral tumor injection exhibited a more differentiated phenotype, higher expression of MHC-I, compared to those not receiving immunotherapy **(Fig. 25)**. Resected tumors were also cultured for growth analysis. Tumors from mice, which received NK immunotherapy, had a much slower growth rate compared to mice under conditions not receiving immunotherapy **(Table 9)**. Once tumors were grown in culture, ^{51}Cr release assay was conducted to measure the susceptibility of these cells to

NK cell-mediated lysis. Tumors from mice that received NK immunotherapy were more resistant to NK cell-mediated lysis, whereas mice that did not receive the treatment were significantly more susceptible to NK cell mediated lysis, indicated their maintained stem-like feature **(Fig. 26)**.

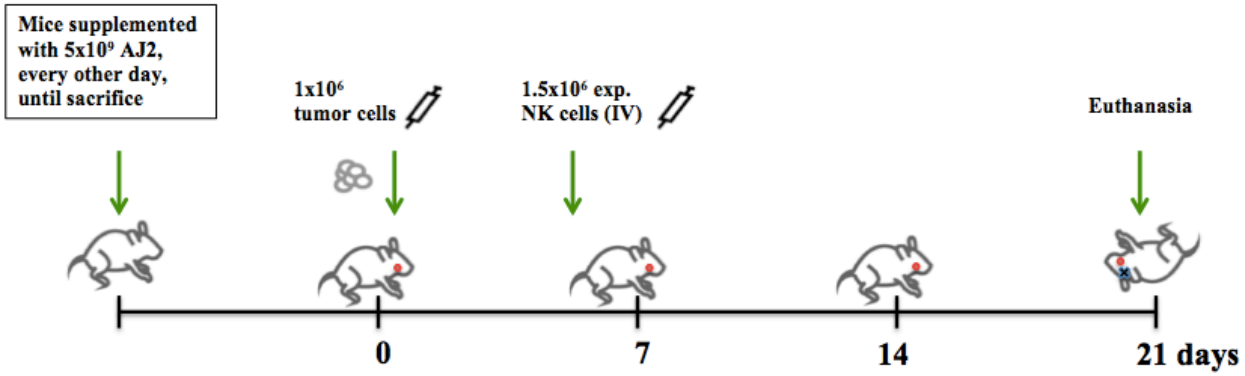

Figure 12. Experimental outline of probiotic supplementation in combination with NK immunotherapy for OSCSCs orthotopically implanted BLT mice.

Prior to tumor implantation, selected mice were fed $5x10^9$ AJ2 bacteria (the combination of 8 probiotic strains listed above) every other day, beginning one week prior to tumor implantation. This adjuvant therapy was continued every other day until the day of sacrifice. For each mouse, lyophilized AJ2 was resuspended in 200 µL of fat free milk, and fed to them via pipetting. Human oral squamous carcinoma stem cells (OSCSCs) were orthotopically injected into the floor of the mouth of hu-BLT mice. Following injection of tumor cells, all mice were continuously monitored for disease progression, every other day. Seven days after tumor implantation, selected hu-BLT mice received $1.5x10^6$ human, osteoclast-expanded NK cells via tail vein (IV) injection. Mice were observed for overall signs of morbidity, such as loss of weight, ruffled fur, hunched posture, and immobility. Mice were sacrificed 3 weeks following initial tumor implantation.

BONE MARROW

A

BM Day 0 CD45+	CD16+56	CD3	HLADR+CD11b
AJ2 control	0.91	2.14	10.2
OSCSCs	1.54	2.12	11.1
OSCSCs+NK	1.45	2.36	15.7
OSCSCs+AJ2	1.83	1.79	11.2
OSCSCs+NK+AJ2	2.51	5.98	16.1

B

BM Day 11 CD45+	CD16+56	CD3+	CD3+ CD8+
AJ2 control	67.4	8.32	4.70
OSCSCs	63.1	6.31	4.43
OSCSCs+NK	54.5	15.22	8.70
OSCSCs+AJ2	57.5	5.22	3.30
OSCSCs+NK+AJ2	48.5	37.02	15.8

Table 2: Human immune cell populations present in the bone marrow of hu-BLT mice.

Hu-BLT mice were treated as described in Figure 12. Following euthanasia, femurs were harvested and bone marrow cells were flushed out using RPMI medium supplemented with 10%FBS. Surface expression of CD45, CD3, CD16, CD56, HLADR, and/or CD11b was conducted using FITC, PE and/or PE-Cy5 conjugated antibodies and assessed via flow cytometry. Cells were gated within the human CD45 positive population and isotype control antibodies were used as controls **(A)**. Bone marrow cells were cultured at $1x10^6$ cells/mL and supplemented with IL-2 (1000 units/mL) on day 0, day 3, day 6, and day 11. Flow cytometry was conducted on day 11, using FITC, PE, and/or PE-Cy5 conjugated antibodies against CD45, CD3, CD16, CD56, or CD8. Cells were gated within the human CD45 positive population and isotype control antibodies were used as controls **(B)**.

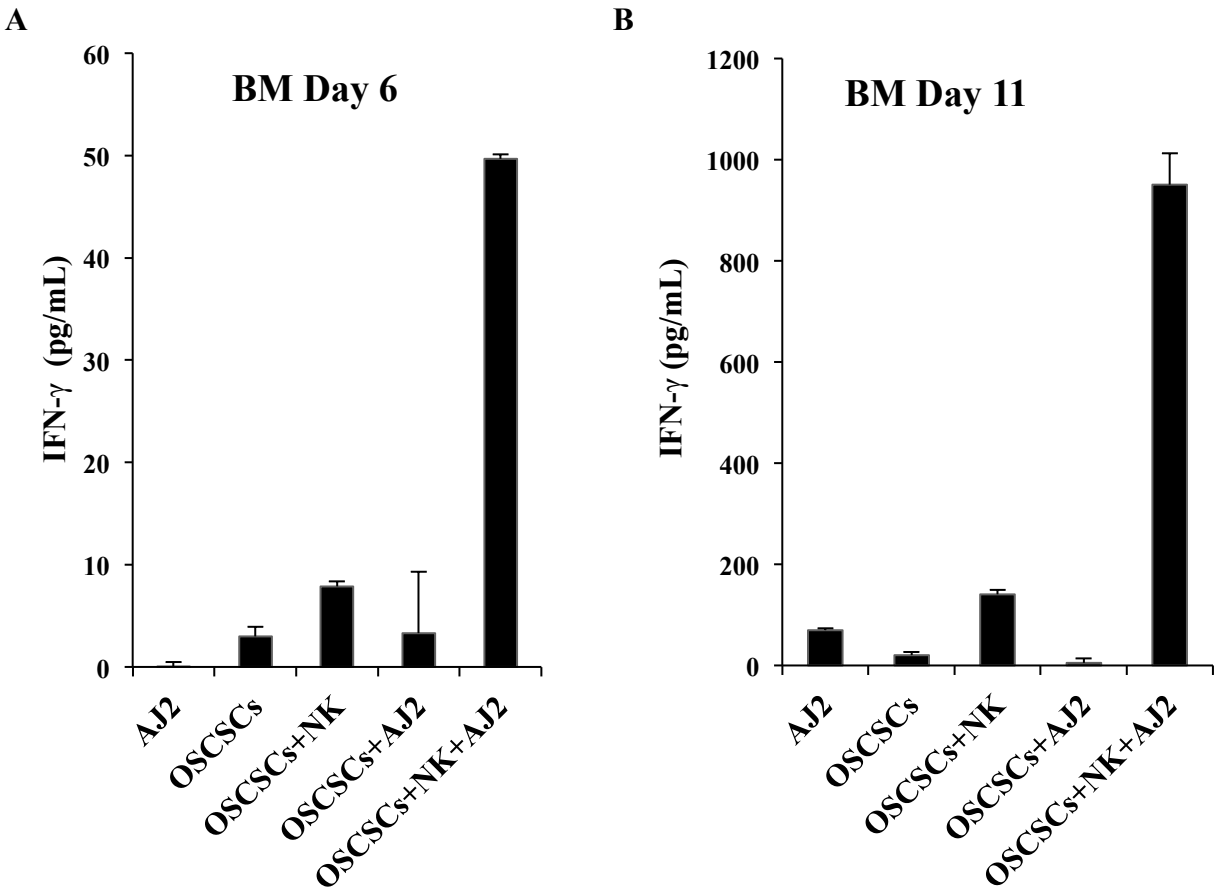

Figure 13: IFN-γ secretion of IL-2 activated bone marrow cells from hu-BLT mice.

Hu-BLT mice were treated as described in Figure 12. Following euthanasia, femurs were harvested and bone marrow cells were flushed out using RPMI medium supplemented with 10%FBS. Bone marrow cells were cultured at $1x10^6$ cells/mL and supplemented with IL-2 (1000 units/mL) on day 0. Supernatants were collected at days 3, 6, and 11. Cells were then resuspended at $1x10^6$ cells/mL and supplemented with IL-2 (1000 units/mL) for each culture timepoint. IFN-γ secretion levels were determined for day 6 **(A)** and day 11 **(B)** supernatants using human IFN-γ ELISA.

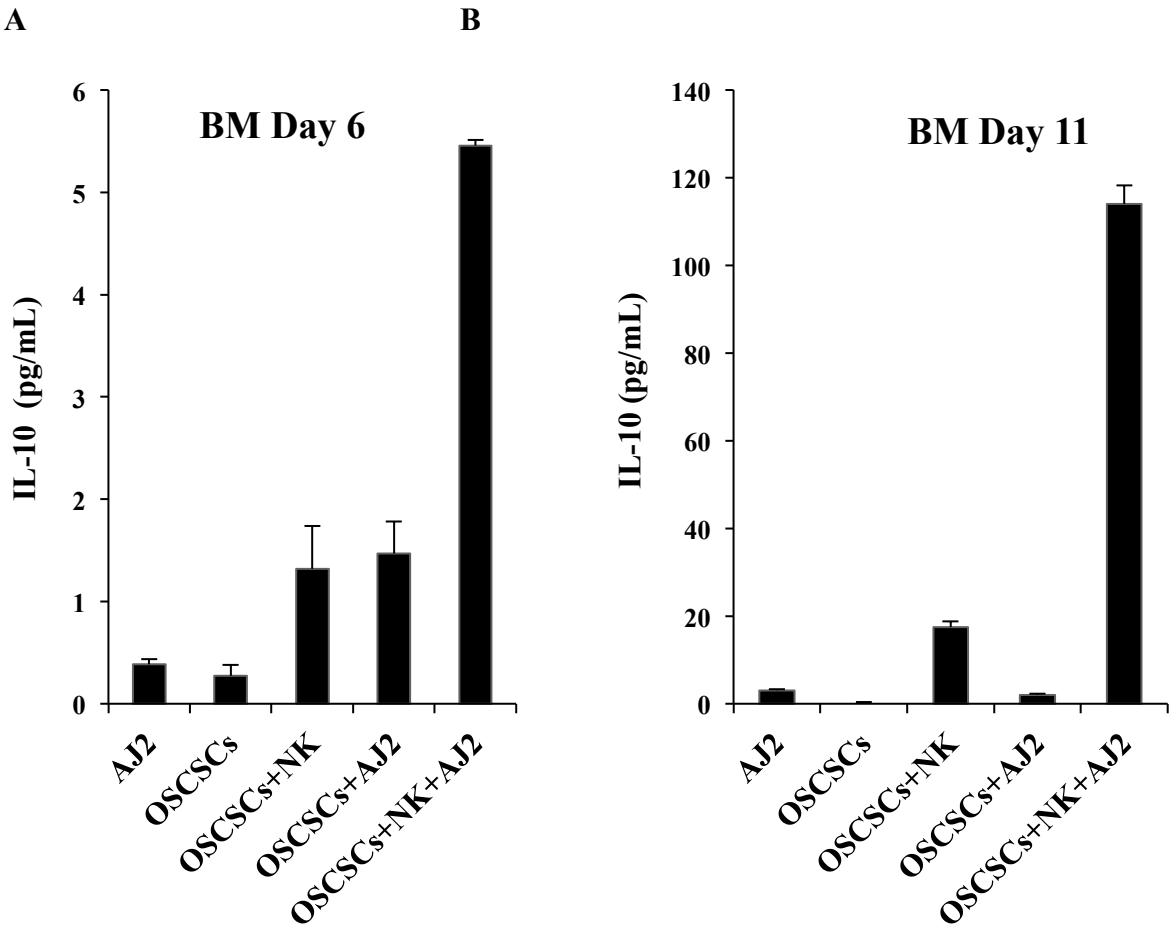

Figure 14: IL-10 secretion of IL-2 activated bone marrow cells from hu-BLT mice.

Hu-BLT mice were treated as described in Figure 12. Following euthanasia, femurs were harvested and bone marrow cells were flushed out using RPMI medium supplemented with 10%FBS. Bone marrow cells were cultured at $1x10^6$ cells/mL and supplemented with IL-2 (1000 units/mL) on day 0. Supernatants were collected at days 3, 6, and 11. Cells were then resuspended at $1x10^6$ cells/mL and supplemented with IL-2 (1000 units/mL) for each culture timepoint. IL-10 secretion levels for day 6 **(A)** and day 11 **(B)** supernatants using human IL-10 ELISA.

PERIPHERAL BLOOD

PBMCs Day 0 CD45+	CD16+56	CD3
AJ2 control	9.67 (3.41)	66.0
OSCSCs	28.2 (8.97)	44.6
OSCSCs+NK	12.4 (4.46)	67.6
OSCSCs+AJ2	20.4 (7.57)	50.2
OSCSCs+NK+AJ2	10.0 (4.64)	72.8

Table 3: Human immune cell populations present in the PBMCs of hu-BLT mice.

Hu-BLT mice were treated as described in Figure 12. Following euthanasia, blood was collected from the mice and PBMCs were separated using Ficoll-Hypaque centrifugation. Surface expression of CD45, CD3, CD16, and CD56 was conducted using FITC, PE and/or PE-Cy5 conjugated antibodies and assessed via flow cytometry. Cells were gated within the human CD45 positive population and isotype control antibodies were used as controls.

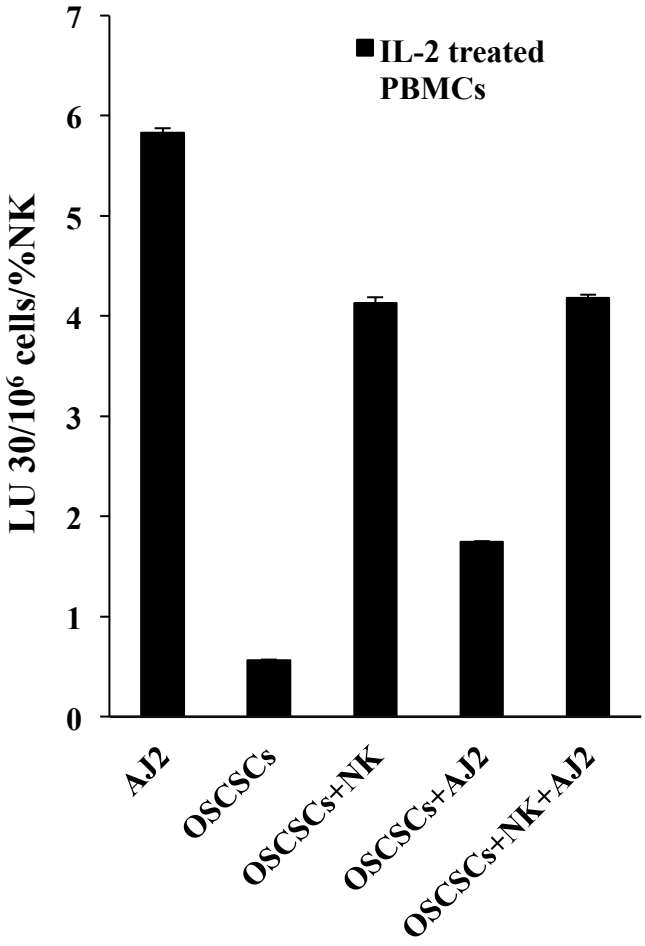

Figure 15: Cell-mediated cytotoxicity of IL-2 activated PBMCs from hu-BLT mice.

Hu-BLT mice were treated as described in Figure 12. Following euthanasia, blood was collected from the mice and PBMCs were separated using Ficoll-Hypaque centrifugation. PBMCs were cultured at $0.4x10^6$ cells/mL and supplemented with IL-2 (1000 units/mL) on day 0, 3 and 7. Cytotoxic function of PBMCs was measured on day 7 using a standard 4-hour ^{51}Cr release assay against radioactively labeled OSCSCs (target cells). Lytic units (LU $30/10^6$) were determined as described in the Materials and Methods.

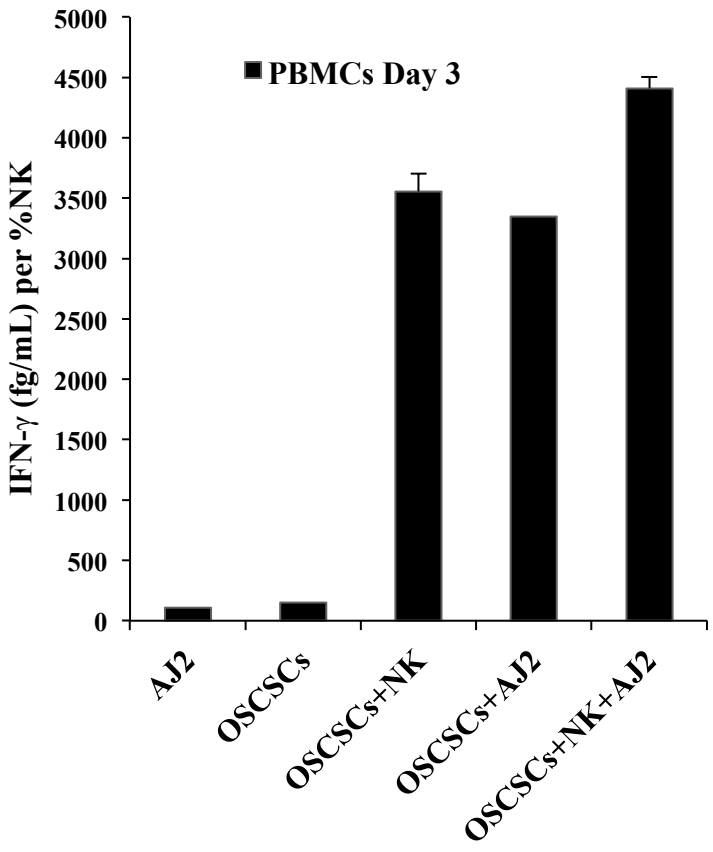

Figure 16: IFN-γ secretion of IL-2 activated PBMCs from hu-BLT mice.

Hu-BLT mice were treated as described in Figure 12. Following euthanasia, blood was collected from the mice and PBMCs were separated using Ficoll-Hypaque centrifugation. PBMCs were cultured at $0.4x10^6$ cells/mL and supplemented with IL-2 (1000 units/mL) on day 0. Supernatants were collected at day 3 and cells were again resuspended at $0.4x10^6$ cells/mL and supplemented with IL-2 (1000 units/mL). IFN-γ secretion levels were determined for supernatants using human IFN-γ ELISA.

A

Sera (pg/mL)	GM-CSF	IFN-γ	IL-10	IL-12p70	IL-13	IL-17A	IL-1β	IL-2	IL-21	IL-4	IL-23	IL-5	IL-6	IL-7	IL-8	TNF-α
AJ2 control	0	1	1	2	0	4	0	4	0	0	0	0	0	4	14	4
OSCSCs	19	5	2	1	0	3	0	0	0	0	0	3	4	2	329	12
OSCSCs+NK	15	8	5	2	5	10	1	0	5	3	55	0	3	3	32	8
OSCSCs+AJ2	0	2	13	2	0	2	0	0	0	0	0	0	0	3	139	9
OSCSCs+NK+AJ2	48	21	13	9	7	17	7	3	7	13	400	1	3	6	6	5

B

Sera (pg/mL)	ITAC	FRACTALKINE	MIP-3α	MIP-1α	MIP-1β
AJ2 control	37	0	0	0	7
OSCSCs	101	0	46	0	10
OSCSCs+NK	20	69	11	11	10
OSCSCs+AJ2	41	0	2	0	11
OSCSCs+NK+AJ2	17	249	16	23	16

Table 4: Cytokine and chemokine profiles of sera samples collected from the cardiac blood of hu-BLT mice post-sacrifice.

Hu-BLT mice were treated as described in Figure 12. Following euthanasia, sera were harvested from cardiac blood. Multiplex array analysis was conducted with sera samples to measure cytokines **(A)** and chemokines **(B)**. Analysis was performed using a MAGPIX Luminex multiplex instrument and data was analyzed using the proprietary software (xPONENT 4.2).

SPLEEN

A

Spleen Day 0 CD45+ (A gate)	CD16+56	CD3
AJ2 control	0.98	55.8
OSCSCs	2.86	38.2
OSCSCs+NK	0.81	64.1
OSCSCs+AJ2	3.66	52.1
OSCSCs+NK+AJ2	1.50	69.9

B

Spleen Day 11 CD45+	CD3+	CD3+ CD8+
AJ2 control	40.2	28.2
OSCSCs	34.61	19.8
OSCSCs+NK	73.0	39.2
OSCSCs+AJ2	14.12	11.1
OSCSCs+NK+AJ2	81.3	50.2

Table 5: Human immune cell populations present in the splenocytes of hu-BLT mice.

Hu-BLT mice were treated as described in Figure 12. Following euthanasia, spleens were harvested, dissociated, filtered for single-cell suspension. Surface expression of CD45, CD3, CD16 and/or CD56 was conducted using FITC, PE and/or PE-Cy5 conjugated antibodies and assessed via flow cytometry. Cells were gated within the human CD45 positive population and isotype control antibodies were used as controls **(A)**. Splenocytes were cultured at $1x10^6$ cells/mL and supplemented with IL-2 (1000 units/mL) on day 0, day 3, day 6, and day 11. Flow cytometry was conducted on day 11, using FITC, PE, and/or PE-Cy5 conjugated antibodies against CD45, CD3, or CD8. Cells were gated within the human CD45 positive population and isotype control antibodies were used as controls **(B)**.

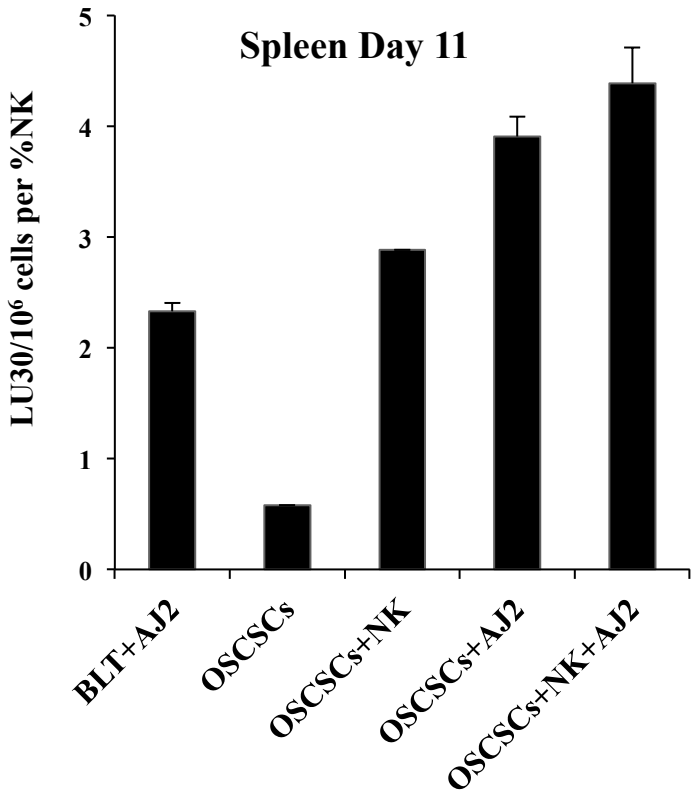

Figure 17: Cell-mediated cytotoxicity of IL-2 activated splenocytes from hu-BLT mice.

Hu-BLT mice were treated as described in Figure 12. Following euthanasia, spleens were harvested, dissociated, filtered for single-cell suspension. Splenocytes were cultured at $1x10^6$ cells/mL and supplemented with IL-2 (1000 units/mL) on day 0. Supernatants were collected at days 3, 6, and 11. Cells were then resuspended at $1x10^6$ cells/mL and supplemented with IL-2 (1000 units/mL) for each culture timepoint. Cytotoxic function of IL-2 treated splenocytes was measured on day 11 using a standard 4-hour ^{51}Cr release assay against radioactively labeled OSCSCs (target cells). Lytic units (LU $30/10^6$) were determined as described in the Materials and Methods.

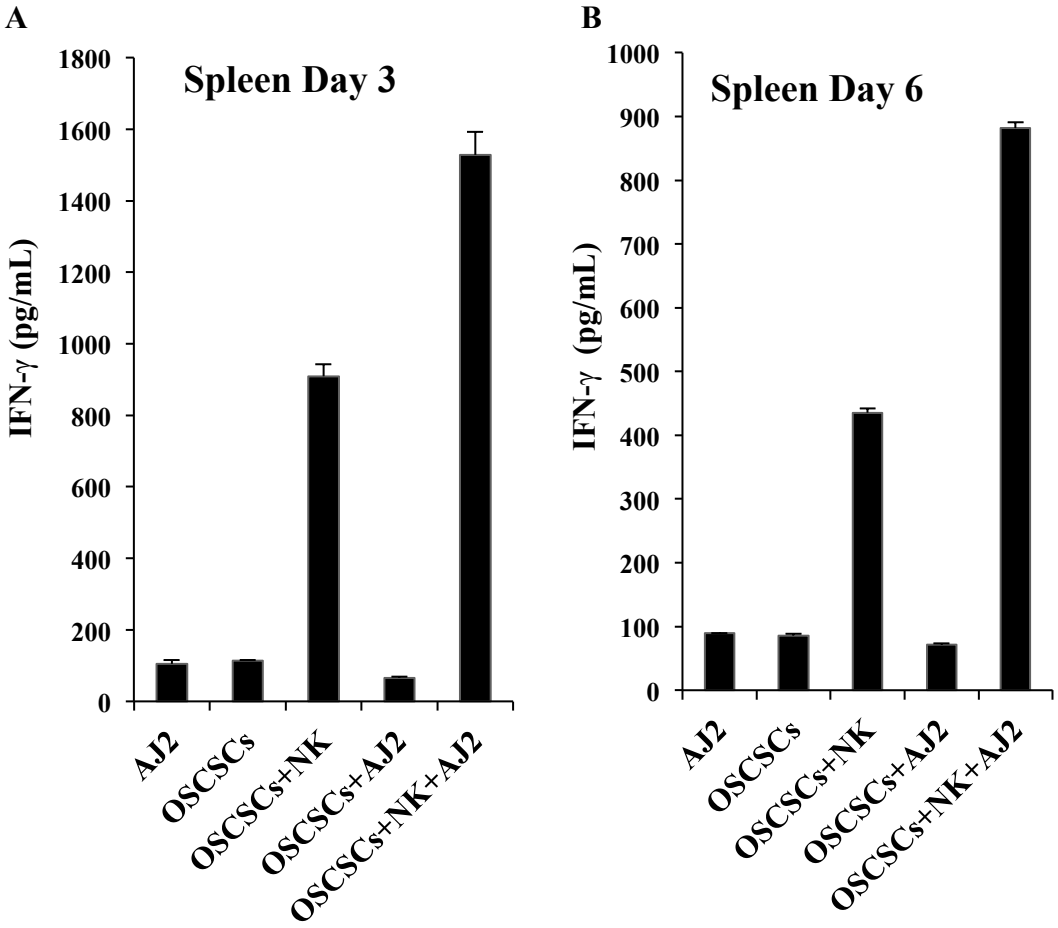

Figure 18: IFN-γ secretion of IL-2 activated splenocytes from hu-BLT mice.

Hu-BLT mice were treated as described in Figure 12. Following euthanasia, spleens were harvested, dissociated, filtered for single-cell suspension. Splenocytes were cultured at $1x10^6$ cells/mL and supplemented with IL-2 (1000 units/mL) on day 0. Supernatants were collected at days 3, 6, and 11. Cells were then resuspended at $1x10^6$ cells/mL and supplemented with IL-2 (1000 units/mL) for each culture timepoint. IFN-γ secretion levels were determined for day 3 **(A)**, day 6 **(B)**, and day 11 **(C, next page)** supernatants using human IFN-γ ELISA.

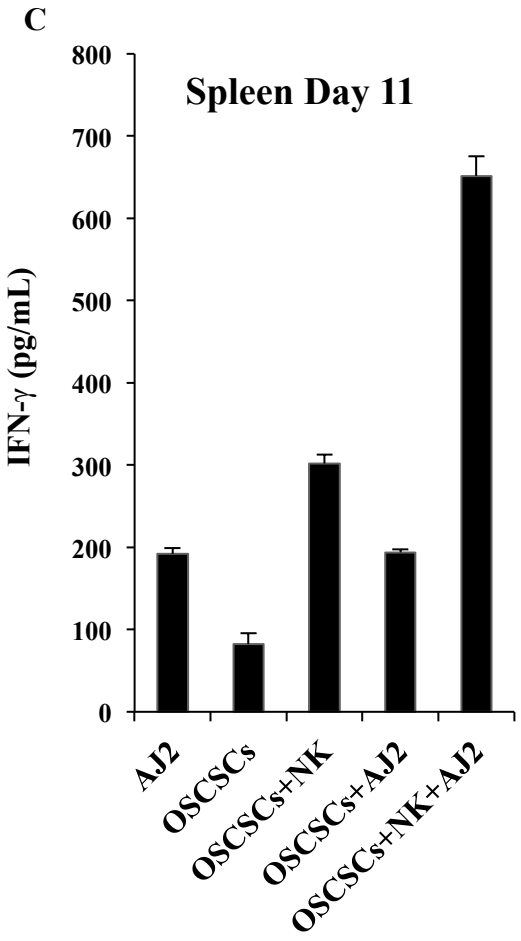

Figure 18 (continued): IFN-γ secretion of IL-2 activated splenocytes from hu-BLT mice.

Hu-BLT mice were treated as described in Figure 12. Following euthanasia, spleens were harvested, dissociated, filtered for single-cell suspension. Splenocytes were cultured at $1x10^6$ cells/mL and supplemented with IL-2 (1000 units/mL) on day 0. Supernatants were collected at days 3, 6, and 11. Cells were then resuspended at $1x10^6$ cells/mL and supplemented with IL-2 (1000 units/mL) for each culture timepoint. IFN-γ secretion levels were determined for day 3 **(A, previous page)**, day 6 **(B, previous page)**, and day 11 **(C)** supernatants using human IFN-γ ELISA.

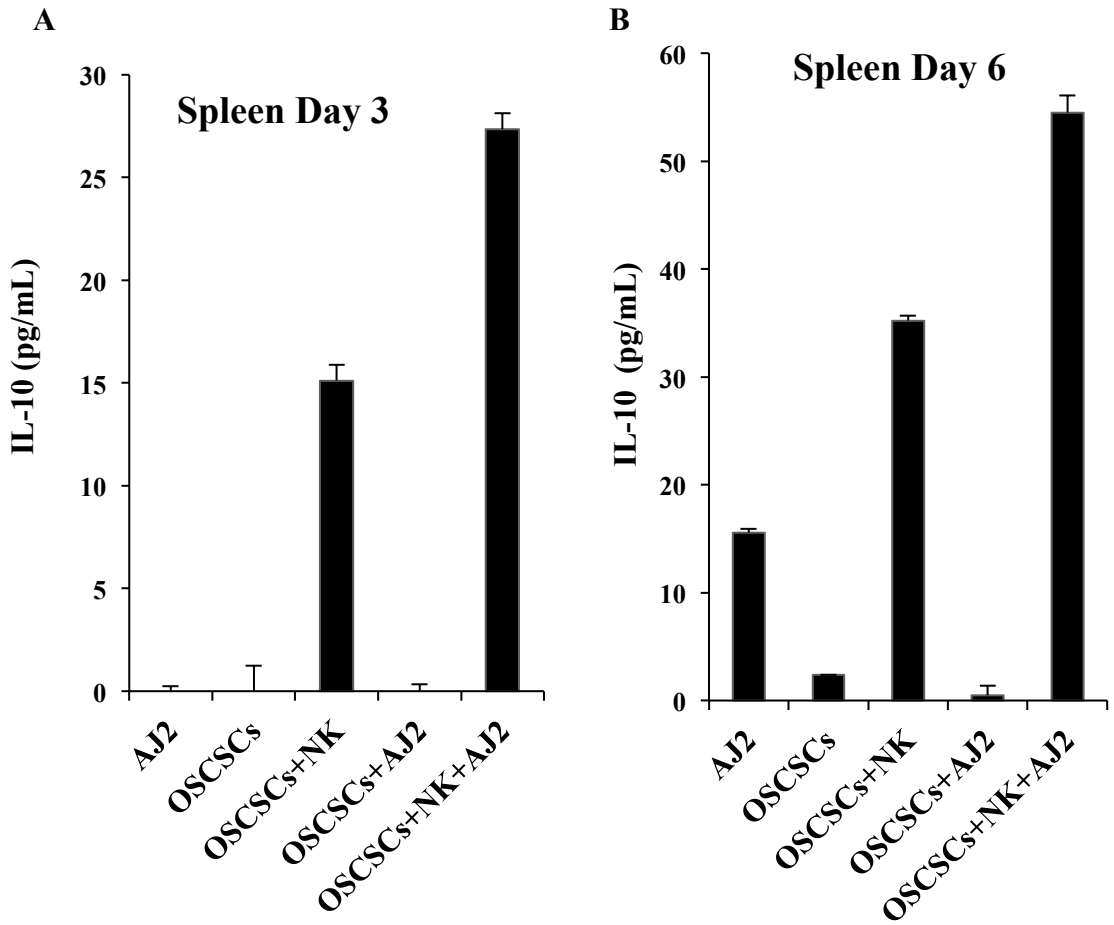

Figure 19: IL-10 secretion of IL-2 activated splenocytes from hu-BLT mice.

Hu-BLT mice were treated as described in Figure 12. Following euthanasia, spleens were harvested, dissociated, filtered for single-cell suspension. Splenocytes were cultured at $1x10^6$ cells/mL and supplemented with IL-2 (1000 units/mL) on day 0. Supernatants were collected at days 3, 6, and 11. Cells were then resuspended at $1x10^6$ cells/mL and supplemented with IL-2 (1000 units/mL) for each culture timepoint. IL-10 secretion levels were determined for day 3 **(A)** and day 6 **(B)** supernatants using human IL-10 ELISA.

A

Spleen Day 3	IL-6	IFN-γ	GM-CSF	TNF-α	IL-8	IL-10
AJ2 control	74	250	103	52	2418	5
OSCSCs	134	263	106	56	5832	5
OSCSCs+NK	1342	393	151	64	11227	10
OSCSCs+AJ2	23	230	68	49	947	2
OSCSCs+NK+AJ2	1332	585	164	74	N/A	16

B

Spleen Day 6	IL-6	IFN-γ	GM-CSF	TNF-α	IL-8	IL-10
AJ2 control	24	244	103	51	672	13
OSCSCs	57	245	104	53	1613	6
OSCSCs+NK	242	328	238	56	4878	25
OSCSCs+AJ2	14	226	72	47	283	3
OSCSCs+NK+AJ2	178	381	229	55	4591	29

Table 6: Cytokine secretion profile of IL-2 activated splenocytes from hu-BLT mice.

Hu-BLT mice were treated as described in Figure 12. Following euthanasia, spleens were harvested, dissociated, filtered for single-cell suspension. Splenocytes were cultured at $1x10^6$ cells/mL and supplemented with IL-2 (1000 units/mL) on day 0. Supernatants were collected at days 3, 6, and 11. Cells were then resuspended at $1x10^6$ cells/mL and supplemented with IL-2 (1000 units/mL) for each culture timepoint. Cytokine secretion levels were determined for day 3 **(A)** and day 6 **(B)** supernatants using multiplex array analysis. Analysis was performed using a MAGPIX Luminex multiplex instrument and data was analyzed using the proprietary software (xPONENT 4.2).

CD3+ SPLENOCYTES

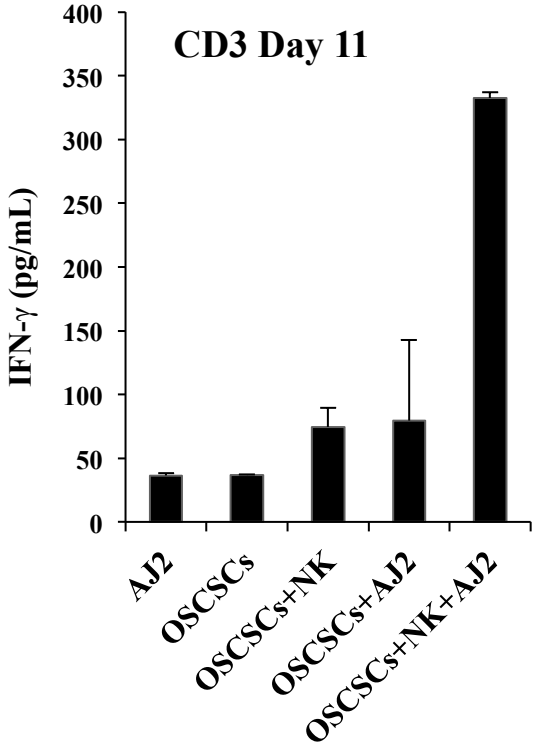

Figure 20: IFN-γ secretion of IL-2 activated CD3+ T cells, positively selected from splenocytes of hu-BLT mice.

Hu-BLT mice were treated as described in Figure 12. Following euthanasia, spleens were harvested, dissociated, filtered for single-cell suspension. Splenocytes underwent CD3 positive selection, and purified T cells were cultured at $1x10^6$ cells/mL and supplemented with IL-2 (1000 units/mL) on day 0. Supernatants were collected at days 3, 6, and 11. Cells were then resuspended at $1x10^6$ cells/mL and supplemented with IL-2 (1000 units/mL) for each culture timepoint. IFN-γ secretion levels were determined for day 11 supernatants using human IFN-γ ELISA.

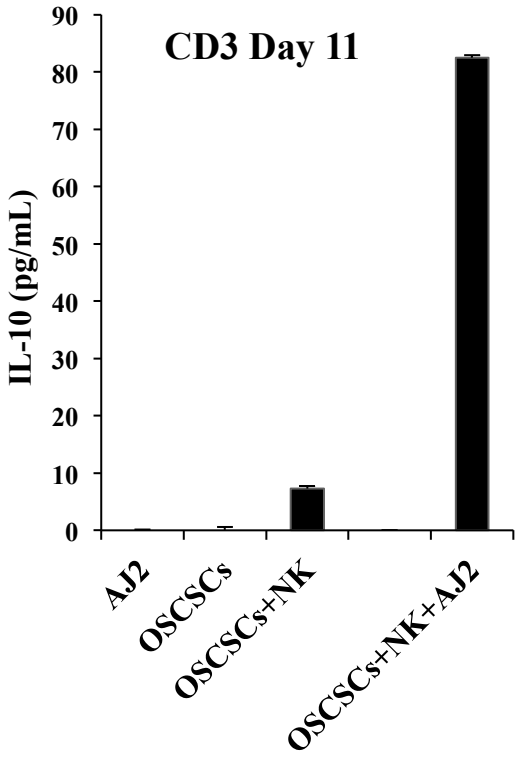

Figure 21: IL-10 secretion of IL-2 activated CD3+ T cells, positively selected from splenocytes of hu-BLT mice.

Hu-BLT mice were treated as described in Figure 12. Following euthanasia, spleens were harvested, dissociated, filtered for single-cell suspension. Splenocytes underwent CD3 positive selection, and purified T cells were cultured at $1x10^6$ cells/mL and supplemented with IL-2 (1000 units/mL) on day 0. Supernatants were collected at days 3, 6, and 11. Cells were then resuspended at $1x10^6$ cells/mL and supplemented with IL-2 (1000 units/mL) for each culture timepoint. IL-10 secretion levels were determined for day 11 supernatants using human IL-10 ELISA.

FLOW THROUGH (CD3 DEPLETED SPLENOCYTES)

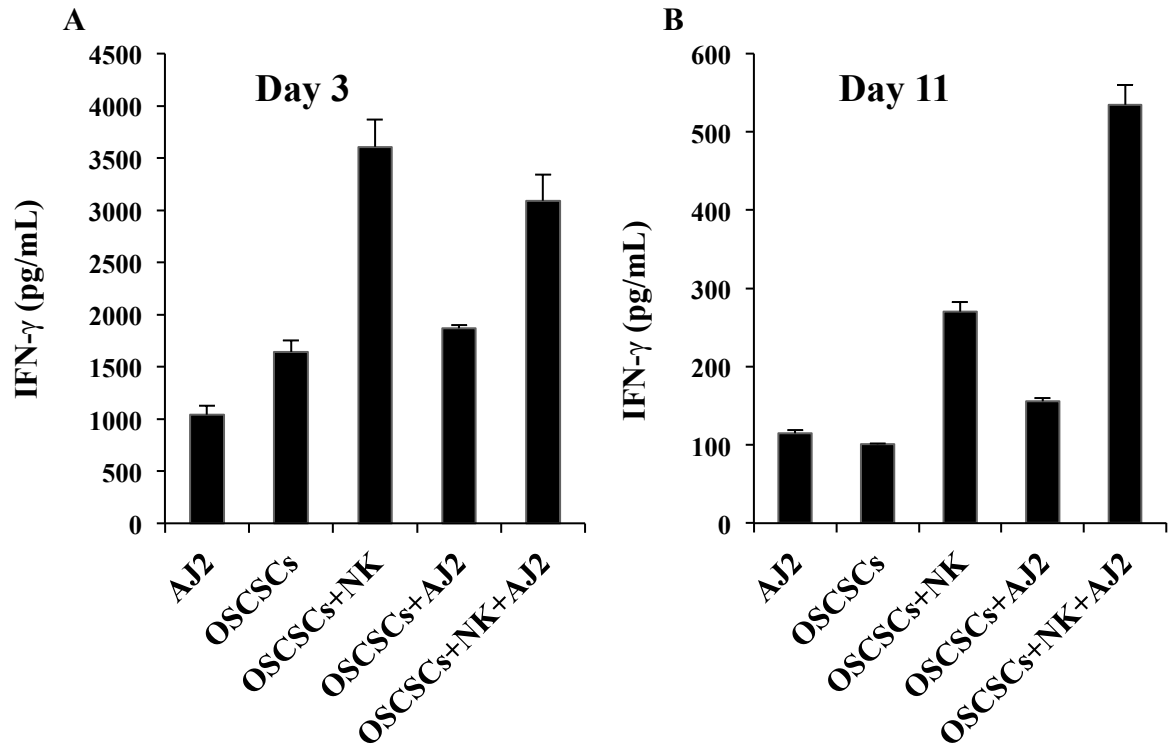

Figure 22: IFN-γ secretion of IL-2 activated CD3 depleted splenocytes from hu-BLT mice.

Hu-BLT mice were treated as described in Figure 12. Following euthanasia, spleens were harvested, dissociated, filtered for single-cell suspension. Splenocytes were depleted of CD3+ cells and cultured at $1x10^6$ cells/mL, supplemented with IL-2 (1000 units/mL) on day 0. Supernatants were collected at days 3, 6, and 11. Cells were then resuspended at $1x10^6$ cells/mL and supplemented with IL-2 (1000 units/mL) for each culture timepoint. IFN-γ secretion levels were determined for day 3 **(A)** and day 11 **(B)** supernatants using human IFN-γ ELISA.

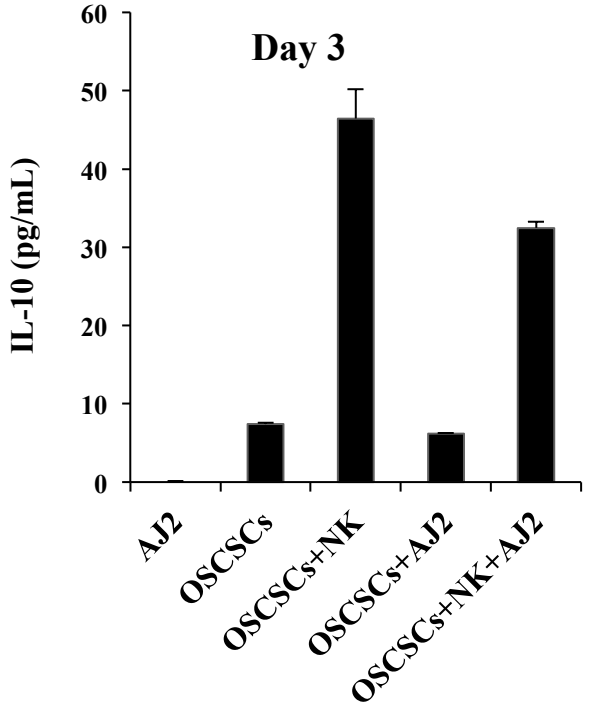

Figure 23: IL-10 secretion of IL-2 activated CD3 depleted splenocytes from hu-BLT mice.

Hu-BLT mice were treated as described in Figure 12. Following euthanasia, spleens were harvested, dissociated, filtered for single-cell suspension. Splenocytes were depleted of CD3+ cells and cultured at $1x10^6$ cells/mL, supplemented with IL-2 (1000 units/mL) on day 0. Supernatants were collected at days 3, 6, and 11. Cells were then resuspended at $1x10^6$ cells/mL and supplemented with IL-2 (1000 units/mL) for each culture timepoint. IL-10 secretion levels were determined for day 11 supernatants using human IL-10 ELISA.

TUMORS

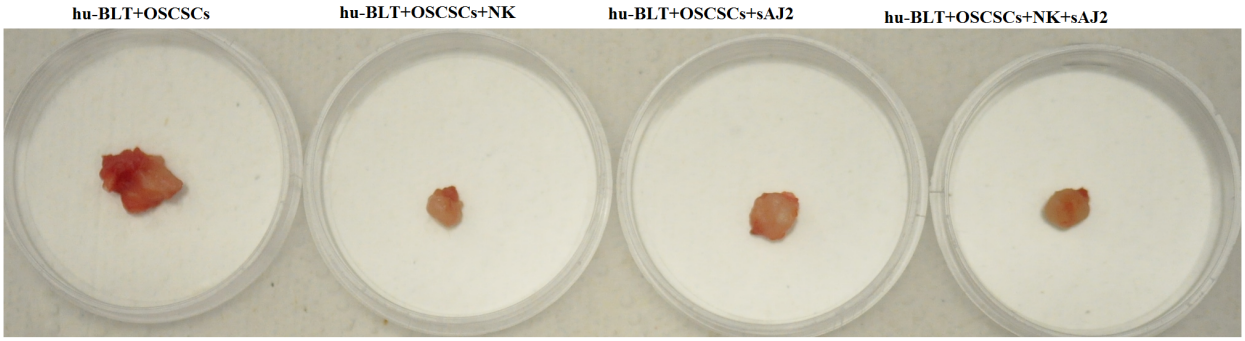

Figure 24: Size analysis of oral tumors resected from hu-BLT mice.

Hu-BLT mice were treated as described in Figure 12. Following euthanasia, oral tumors were harvested and photographed side-by-side.

Tumor Day 0, sac day	Weight (grams)	Day 0 total counts (million cells)
1-AJ2 ctrl	N/A	N/A
2-OSCSCs	0.15	6.9
3-OSCSCs+NK	0.04	2.1
4-OSCSCs+AJ2	0.071	5.2
5-OSCSCs+NK+AJ2	0.062	2.3

Table 7: Measurements of oral tumors resected from hu-BLT mice.

Hu-BLT mice were treated as described in Figure 12. Following euthanasia, oral tumors were harvested and weights of tumors were recorded. Tumor cells were then dissociated and filtered for single-cell suspension. Cell counts were noted as shown in the table above

Tumors Day 0 CD45+	CD3
OSCSCs	56.3
OSCSCs+NK	81.0
OSCSCs+AJ2	76.5
OSCSCs+NK+AJ2	83.7

Table 8: Human immune cell populations present in oral tumors resected from hu-BLT mice.

Hu-BLT mice were treated as described in Figure 12. Following euthanasia, oral tumors were harvested, dissociated, and filtered for single-cell suspension. Flow cytometry was conducted on day 0, using FITC, PE, and/or PE-Cy5 conjugated antibodies against CD45, CD3 to measure immune cell presence within the tumor. Cells were gated within the human CD45 positive population and isotype control antibodies were used as controls.

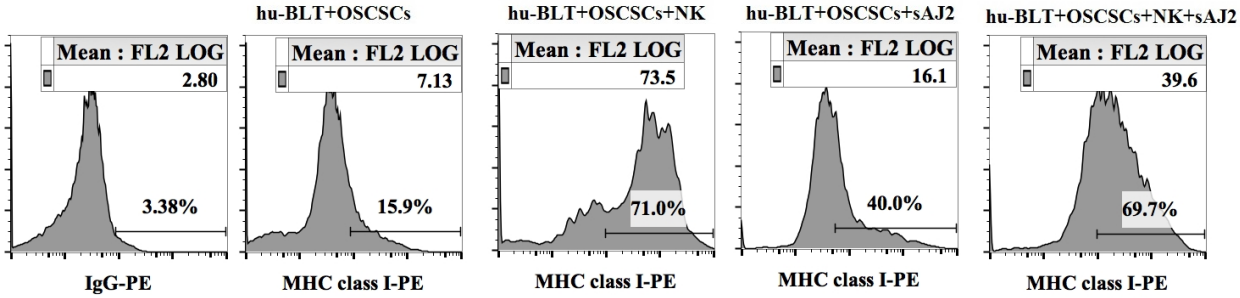

Figure 25: Surface expression of MHC-I on oral tumors resected from hu-BLT mice.

Hu-BLT mice were treated as described in Figure 12. Following euthanasia, oral tumors were harvested, dissociated, and filtered for single-cell suspension. Flow cytometry was conducted on day 0, using PE-conjugated MHC-I antibodies. Isotype control antibodies were used as controls.

Tumors (attached)	Day 7	Day 15
OSCSCs	0.268	0.792
OSCSCs+NK	0.042	0.2
OSCSCs+AJ2	0.216	0.856
OSCSCs+NK+AJ2	0.062	0.3

Table 9: *in vitro* growth analysis of oral tumors resected from hu-BLT mice.

Hu-BLT mice were treated as described in Figure 12. Following euthanasia, oral tumors were harvested, dissociated and filtered for single-cell suspension. Cell for each tumor were cultured at $0.75x10^6$ cells per well at day 0. Cells were detached and counted at day 7, and re-cultured at 10,000 cells for each condition. Cells were again detached and counted at day 15.

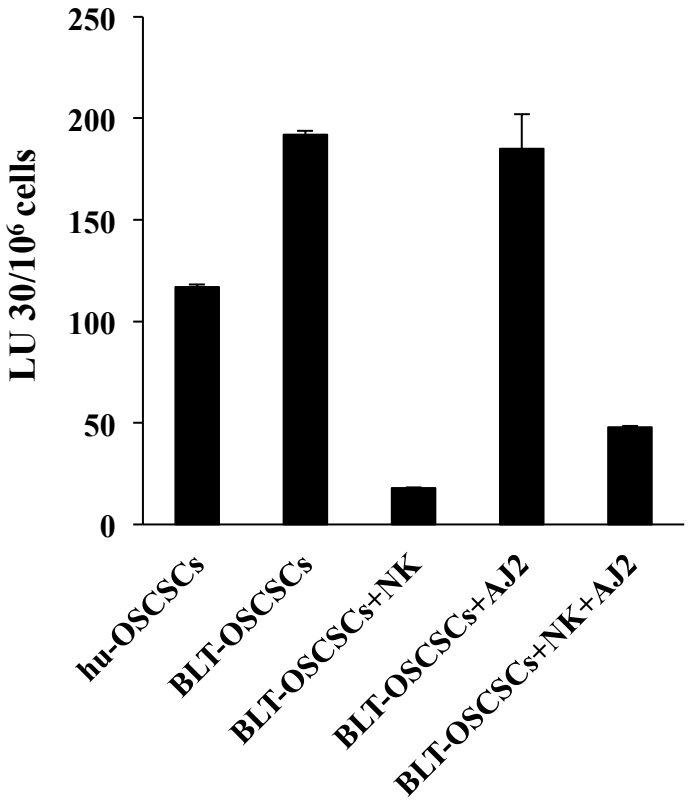

Figure 26: NK-cell mediated cytotoxicity against oral tumors resected from hu-BLT mice.

Hu-BLT mice were treated as described in Figure 12. Following euthanasia, oral tumors were harvested, dissociated and filtered for single-cell suspension. Cell for each tumor were cultured at $0.75x10^6$ cells per well at day 0. Cells were detached at day 7, and re-cultured at 10,000 cells for each condition. On day 15, oral tumor cells were detached and used for experimentation. Tumor sensitivity to NK-cell mediated cytotoxicity was measured using a standard 4-hour ^{51}Cr release assay against freshly isolated and IL-2 (1000 units/mL) activated NK cells. Lytic units (LU $30/10^6$) were determined as described in the Materials and Methods.

DISCUSSION

Our lab has previously shown that cytokines, primarily IFN-γ and TNF-α, secreted by the NK cells are responsible for the increase in differentiation antigens MHC class I, CD54, and B7H1 and decrease in CD44 resulting in the differentiation of both healthy and transformed stem cells, including OSCSCs [8, 9]. This study demonstrates that probiotic bacteria also induce significant split anergy in NK cells, thus resulting in increased cytokine secretion.

sAJ2 is a combination of 8 strains of probiotic bacteria selected for their ability to induce synergistic secretion of IFN-γ when added to IL-2 or IL-2+anti-CD16mAb treated NK cells [9]. The amount of each strain was adjusted to yield a ratio of IFN-γ to IL-10 to that obtained when NK cells are activated with IL-2 or IL-2+anti-CD16mAb without bacteria. This was done in order to obtain a ratio of probiotics closest to when NK cells are activated with IL-2+anti-CD16mAb without bacteria, since this NK treatment provided increased differentiation of the stem cells. This combination of bacterial strains was selected to provide bacterial diversity as well as for its optimal induction of other pro- and anti-inflammatory cytokines and growth factors by the NK cells [9].

Although there was no significant difference observed in the NK cell cytotoxic levels of sAJ2 treatment, significantly augmented cytokine secretion was observed in NK cells treated with sAJ2 probiotic, suggesting a dissociation between cytotoxicity and cytokine secretion functions of NK cells affected by bacteria (Fig. 1 and 2). Based on this project, sAJ2 bacteria treated, split anergized NK cell supernatants also induced greater differentiation and resistance of OSCSCs to NK cell mediated cytotoxicity (another indication of differentiation, since NK cells tend to target stem/stem-like cells and not their more differentiated counterparts) (Fig. 3 and 4). This differentiation of OSCSCs induced by split anergized NK cells treated with sAJ2 is

significantly mediated through the cytokine secretion of IFN-γ and/or TNF-α (Fig. 3-7). Thus, sAJ2 probiotic bacteria treatment of NK cells induces cytokine secretion, further resulting in tumor differentiation, and reduced tumor growth.

To our knowledge, using osteoclasts as feeder cells in combination with IL-2+anti-CD16mAb+sAJ2 is the best strategy to expand large numbers of NK cells with a significant capability to target cancer stem cells when compared to a number of previous strategies (Table 1 and Fig. 11). Our lab has obtained 21,000-132,000 fold expansion on day 20, and 0.3-5.1 million on day 31, with 17-21 population doublings within 4 weeks—a much higher rate than any previously reported NK expansion method (manuscript in prep). Although cytotoxic function of expanded NK cells across studies are difficult to compare due to different types of targets used for assessment, our strategy provides expanded NK cells (which maintain their purity for a long period of time) with significant functionality to target and lyse cancer stem cells, in addition to providing larger amounts of IFN-γ secretion (Fig. 8-10).

Since both autologous and allogeneic NK cells can be expanded using our laboratory's NK expansion protocol, our recent findings show promise in being translated into a therapeutic immunotherapy for cancer patients. Thus, it is all the more crucial that our previous data [6, 24, 93] and current *in vivo* studies indicate that NK cells are the main immune effectors that select and differentiate CSCs, resulting in inhibition of tumor growth and resolution of chronic inflammation during disease progression [24, 64]. We have most recently observed that non-HLA matched oral, pancreatic and melanoma CSCs are able to form substantial tumors in BLT humanized mice that have a fully reconstituted human immune system. In addition, major human immune subsets including NK cells, T cells, B cells and monocytes were present in bone marrow (Table 2), blood (Table 3), spleen (Table 5), and infiltrated tumor microenvironment (Table 8)

(data not shown). Similarly to our previously published *in vitro* data, intravenous injection of expanded NK cells inhibited tumor growth of OSCSCs by differentiating CSCs in humanized mice (Table 7 and 9, Fig. 24-26). Similar to our *in vitro* findings, tumors differentiated through NK immunotherapy expressed higher levels of MHC-I (Fig. 25), were more resistant to NK cell mediated cytotoxicity (Fig. 26) and grew at a much slower rate (Table 7 and 9, Fig. 24). These results clearly showed that NK cell-induced tumor differentiation is important in the limitation of tumor growth and aggressiveness. It also showed that probiotic bacteria, combined with NK activated cytokines and osteoclasts as feeder cells provide a condition for NK cells to promote tumor differentiation.

The use of NK immunotherapy supplemented with AJ2 also enhanced the function of NK cells in various immune tissue compartments. Various tissue compartments of hu-BLT mice receiving NK immunotherapy secreted high levels of IFN-γ and IL-10 (Fig. 14B, 16, 18, 19, 21-23 and Table 6). Meanwhile, with NK immunotherapy in combination with AJ2 supplementation, there was a significant increase in cytokine secretion levels as compared to the NK immunotherapy alone (Fig. 13, 14, 18-21 and Table 4 and 6). Mice receiving NK immunotherapy treatment had significantly improved cytotoxic function compared to tumor-bearing alone condition, which demonstrated significantly reduced cytotoxic function in both cultured PBMCs (Fig. 15) and splenocytes (Fig. 17). Similar to the tumor alone condition, NK cells of cancer patients also show lack of function both in terms of cytokine secretion and cytotoxicity. Meanwhile, similar to the hu-BLT healthy control group, healthy human PBMCs, when activated with IL-2 alone, demonstrate low cytokine secretion and a high level of cytotoxicity (Fig. 15 and 16). The tumor-bearing, probiotic supplementation control group exhibits the split anergized phenotype, in which cytotoxicity is reduced, but there is augmented

IFN- γ secretion (Fig. 15 and 16). Meanwhile, mice that receive NK immunotherapy following tumor injections demonstrate both cytotoxic as well as cytokine secretory functions (Fig. 15 and 16). This demonstrates the continued *in vivo* potency of *ex vivo* expanded NK cells and their ability to select and differentiate cancer stem-like tumors in the BLT humanized mouse model, in combination with probiotic supplementation.

CONCLUSION

In conclusion, NK cells expanded using our laboratory's novel strategy can select and differentiate CSCs both in *in vitro* and *in vivo* systems. The use of NK immunotherapy supplemented with AJ2 induced higher percentages of NK cells and T cells, and enhanced the functions of NK cells, especially their cytokine secreting ability. It was also discovered that NK immunotherapy could select and differentiate oral tumors in the presence of probiotic bacteria. These findings provide a vital translational research foundation. We now understand the remarkable effects of our NK immunotherapy in humanized mice, most notably its ability to prevent tumor growth and differentiate tumors. Further studies include bringing these findings into the clinical setting, through Phase I clinical trials testing the effects of our NK immunotherapy, and the use of probiotic supplementation as an adjuvant therapy to cancer treatment, or as a cancer preventative measure. It would also be interesting to investigate the use of probiotic supplementation in combination with chemotherapy or immunotherapy. NK cells, due to their unique functional ability to target, kill and differentiate CSCs, which are capable of metastasis and cancer regeneration, may hold the key to preventing cancer relapse in patients. Therefore, it is important that further research focus on the field of NK cells in cancer immunology. This breakthrough method of NK expansion may provide the answer for optimized adoptive NK immunotherapy.

REFERENCES

1. Palmer, J.M., et al., *Clinical relevance of natural killer cells following hematopoietic stem cell transplantation.* J Cancer, 2013. **4**(1): p. 25-35.
2. Fildes, J.E., N. Yonan, and C.T. Leonard, *Natural killer cells and lung transplantation, roles in rejection, infection, and tolerance.* Transpl Immunol, 2008. **19**(1): p. 1-11.
3. Farag, S.S. and M.A. Caligiuri, *Human natural killer cell development and biology.* Blood Rev, 2006. **20**(3): p. 123-37.
4. Trinchieri, G., *Biology of natural killer cells.* Adv Immunol, 1989. **47**: p. 187-376.
5. Lanier, L.L., *NK cell recognition.* Annu Rev Immunol, 2005. **23**: p. 225-74.
6. Tseng, H.C., et al., *Increased lysis of stem cells but not their differentiated cells by natural killer cells; de-differentiation or reprogramming activates NK cells.* PLoS One, 2010. **5**(7): p. e11590.
7. Jewett, A., et al., *Natural killer cells as effectors of selection and differentiation of stem cells: role in resolution of inflammation.* J Immunotoxicol, 2014. **11**(4): p. 297-307.
8. Tseng, H.C., et al., *Induction of Split Anergy Conditions Natural Killer Cells to Promote Differentiation of Stem Cells through Cell-Cell Contact and Secreted Factors.* Front Immunol, 2014. **5**: p. 269.
9. Bui, V.T., et al., *Augmented IFN-gamma and TNF-alpha Induced by Probiotic Bacteria in NK Cells Mediate Differentiation of Stem-Like Tumors Leading to Inhibition of Tumor Growth and Reduction in Inflammatory Cytokine Release; Regulation by IL-10.* Front Immunol, 2015. **6**: p. 576.
10. Moretta, L., et al., *Human natural killer cells: origin, receptors, function, and clinical applications.* Int Arch Allergy Immunol, 2014. **164**(4): p. 253-64.
11. Larsen, S.K., Y. Gao, and P.H. Basse, *NK cells in the tumor microenvironment.* Crit Rev Oncog, 2014. **19**(1-2): p. 91-105.
12. Burke, S., et al., *New views on natural killer cell-based immunotherapy for melanoma treatment.* Trends Immunol, 2010. **31**(9): p. 339-45.
13. Imai, K., et al., *Natural cytotoxic activity of peripheral-blood lymphocytes and cancer incidence: an 11-year follow-up study of a general population.* Lancet, 2000. **356**(9244): p. 1795-9.
14. Hersey, P., et al., *Low natural-killer-cell activity in familial melanoma patients and their relatives.* Br J Cancer, 1979. **40**(1): p. 113-22.
15. Castriconi, R., et al., *Transforming growth factor beta 1 inhibits expression of NKp30 and NKG2D receptors: consequences for the NK-mediated killing of dendritic cells.* Proc Natl Acad Sci U S A, 2003. **100**(7): p. 4120-5.
16. Balsamo, M., et al., *Melanoma-associated fibroblasts modulate NK cell phenotype and antitumor cytotoxicity.* Proc Natl Acad Sci U S A, 2009. **106**(49): p. 20847-52.
17. Gubbels, J.A., et al., *MUC16 provides immune protection by inhibiting synapse formation between NK and ovarian tumor cells.* Mol Cancer, 2010. **9**: p. 11.
18. Pietra, G., et al., *Melanoma cells inhibit natural killer cell function by modulating the expression of activating receptors and cytolytic activity.* Cancer Res, 2012. **72**(6): p. 1407-15.

19. Bruno, A., et al., *A think tank of TINK/TANKs: tumor-infiltrating/tumor-associated natural killer cells in tumor progression and angiogenesis.* J Natl Cancer Inst, 2014. **106**(8): p. dju200.
20. Gallois, A., et al., *Reversal of natural killer cell exhaustion by TIM-3 blockade.* Oncoimmunology, 2014. **3**(12): p. e946365.
21. Mirjacic Martinovic, K.M., et al., *Decreased expression of NKG2D, NKp46, DNAM-1 receptors, and intracellular perforin and STAT-1 effector molecules in NK cells and their dim and bright subsets in metastatic melanoma patients.* Melanoma Res, 2014. **24**(4): p. 295-304.
22. Vitale, M., et al., *Effect of tumor cells and tumor microenvironment on NK-cell function.* Eur J Immunol, 2014. **44**(6): p. 1582-92.
23. Magister, S., et al., *Regulation of cathepsins S and L by cystatin F during maturation of dendritic cells.* Eur J Cell Biol, 2012. **91**(5): p. 391-401.
24. Tseng, H.C., N. Cacalano, and A. Jewett, *Split anergized Natural Killer cells halt inflammation by inducing stem cell differentiation, resistance to NK cell cytotoxicity and prevention of cytokine and chemokine secretion.* Oncotarget, 2015. **6**(11): p. 8947-59.
25. Metchnikoff, E., *Essais optimistes*. 1907, Paris: A. Maloine. iii, 438 p.
26. Fuller, R., *PROBIOTICS IN MAN AND ANIMALS.* Journal of Applied Bacteriology, 1989. **66**(5): p. 365-378.
27. Matsuzaki, T. and J. Chin, *Modulating immune responses with probiotic bacteria.* Immunology and cell biology, 2000. **78**(1): p. 67-73.
28. Gill, H.S., et al., *Enhancement of immunity in the elderly by dietary supplementation with the probiotic Bifidobacterium lactis HN019.* The American journal of clinical nutrition, 2001. **74**(6): p. 833-9.
29. Perdigon, G., et al., *Systemic augmentation of the immune response in mice by feeding fermented milks with Lactobacillus casei and Lactobacillus acidophilus.* Immunology, 1988. **63**(1): p. 17-23.
30. Isolauri, E., et al., *Probiotics: effects on immunity.* The American journal of clinical nutrition, 2001. **73**(2 Suppl): p. 444S-450S.
31. Park, J.H., et al., *Encapsulated Bifidobacterium bifidum potentiates intestinal IgA production.* Cellular immunology, 2002. **219**(1): p. 22-7.
32. Fukushima, Y., et al., *Effect of a probiotic formula on intestinal immunoglobulin A production in healthy children.* International journal of food microbiology, 1998. **42**(1-2): p. 39-44.
33. Rautava, S., H. Arvilommi, and E. Isolauri, *Specific probiotics in enhancing maturation of IgA responses in formula-fed infants.* Pediatric research, 2006. **60**(2): p. 221-4.
34. Ustunol, Z. and J.J. Pestka, *Probiotics in health: Their immunomodulatory potential against allergic disorders.* Journal of Animal Science, 2004. **82**: p. 274-274.
35. Fuccio, L., et al., *Effects of Probiotics for the Prevention and Treatment of Radiation-induced Diarrhea.* Journal of Clinical Gastroenterology, 2009. **43**(6): p. 506-513.
36. Ouwehand, A.C., *Antiallergic effects of probiotics.* The Journal of nutrition, 2007. **137**(3 Suppl 2): p. 794S-7S.
37. Fotiadis, C.I., et al., *Role of probiotics, prebiotics and synbiotics in chemoprevention for colorectal cancer.* World Journal of Gastroenterology, 2008. **14**(42): p. 6453-6457.

38. Ozdemir, O., *Various effects of different probiotic strains in allergic disorders: an update from laboratory and clinical data.* Clinical and experimental immunology, 2010. **160**(3): p. 295-304.
39. Dongarra, M.L., et al., *Mucosal immunology and probiotics.* Current allergy and asthma reports, 2013. **13**(1): p. 19-26.
40. Tseng, H.C., et al., *Bisphosphonate-induced differential modulation of immune cell function in gingiva and bone marrow in vivo: role in osteoclast-mediated NK cell activation.* Oncotarget, 2015. **6**(24): p. 20002-25.
41. SUDA, T., N. TAKAHASHI, and T.J. MARTIN, *Modulation of Osteoclast Differentiation.* Endocrine Reviews, 1992. **13**(1): p. 66-80.
42. Tanaka, Y., S. Nakayamada, and Y. Okada, *Osteoblasts and osteoclasts in bone remodeling and inflammation.* Curr Drug Targets Inflamm Allergy, 2005. **4**(3): p. 325-8.
43. Feng, S., et al., *IL-15-activated NK cells kill autologous osteoclasts via LFA-1, DNAM-1 and TRAIL, and inhibit osteoclast-mediated bone erosion in vitro.* Immunology, 2015.
44. Lanier, L.L., *NK cell receptors.* Annu Rev Immunol, 1998. **16**: p. 359-93.
45. London, L., B. Perussia, and G. Trinchieri, *Induction of proliferation in vitro of resting human natural killer cells: IL 2 induces into cell cycle most peripheral blood NK cells, but only a minor subset of low density T cells.* J Immunol, 1986. **137**(12): p. 3845-54.
46. Perussia, B., et al., *Preferential proliferation of natural killer cells among peripheral blood mononuclear cells cocultured with B lymphoblastoid cell lines.* Nat Immun Cell Growth Regul, 1987. **6**(4): p. 171-88.
47. Igarashi, T., et al., *Enhanced cytotoxicity of allogeneic NK cells with killer immunoglobulin-like receptor ligand incompatibility against melanoma and renal cell carcinoma cells.* Blood, 2004. **104**(1): p. 170-7.
48. Rabinowich, H., et al., *Increased proliferation, lytic activity, and purity of human natural killer cells cocultured with mitogen-activated feeder cells.* Cell Immunol, 1991. **135**(2): p. 454-70.
49. Srivastava, S., A. Lundqvist, and R.W. Childs, *Natural killer cell immunotherapy for cancer: a new hope.* Cytotherapy, 2008. **10**(8): p. 775-83.
50. Miller, J.S., et al., *Role of monocytes in the expansion of human activated natural killer cells.* Blood, 1992. **80**(9): p. 2221-9.
51. Gras Navarro, A., A. Björklund, and M. Chekenya, *Therapeutic potential and challenges of Natural killer cells in treatment of solid tumors.* Frontiers in Immunology, 2015. **6**.
52. Fujisaki, H., et al., *Expansion of highly cytotoxic human natural killer cells for cancer cell therapy.* Cancer Res, 2009. **69**(9): p. 4010-7.
53. Alici, E., et al., *Autologous antitumor activity by NK cells expanded from myeloma patients using GMP-compliant components.* Blood, 2008. **111**(6): p. 3155-62.
54. Carlens, S., et al., *A new method for in vitro expansion of cytotoxic human CD3-CD56+ natural killer cells.* Hum Immunol, 2001. **62**(10): p. 1092-8.
55. Berg, M., et al., *Clinical-grade ex vivo-expanded human natural killer cells up-regulate activating receptors and death receptor ligands and have enhanced cytolytic activity against tumor cells.* Cytotherapy, 2009. **11**(3): p. 341-55.
56. Trinchieri, G., et al., *Response of resting human peripheral blood natural killer cells to interleukin 2.* J Exp Med, 1984. **160**(4): p. 1147-69.
57. Garg, T.K., et al., *Highly activated and expanded natural killer cells for multiple myeloma immunotherapy.* Haematologica, 2012. **97**(9): p. 1348-56.

58. Shah, N., et al., *Antigen presenting cell-mediated expansion of human umbilical cord blood yields log-scale expansion of natural killer cells with anti-myeloma activity.* PLoS One, 2013. **8**(10): p. e76781.
59. Robertson, M.J., et al., *Costimulatory signals are required for optimal proliferation of human natural killer cells.* J Immunol, 1993. **150**(5): p. 1705-14.
60. Lanier, L.L., et al., *Interleukin 2 activation of natural killer cells rapidly induces the expression and phosphorylation of the Leu-23 activation antigen.* J Exp Med, 1988. **167**(5): p. 1572-85.
61. Imai, C., S. Iwamoto, and D. Campana, *Genetic modification of primary natural killer cells overcomes inhibitory signals and induces specific killing of leukemic cells.* Blood, 2005. **106**(1): p. 376-83.
62. Lapteva, N., et al., *Large-scale ex vivo expansion and characterization of natural killer cells for clinical applications.* Cytotherapy, 2012. **14**(9): p. 1131-43.
63. Shultz, L.D., et al., *Human cancer growth and therapy in immunodeficient mouse models.* Cold Spring Harb Protoc, 2014. **2014**(7): p. 694-708.
64. Kozlowska, A.K., et al., *Adoptive transfer of osteoclast-expanded natural killer cells for immunotherapy targeting cancer stem-like cells in humanized mice.* Cancer Immunology, Immunotherapy, 2016. **65**(7): p. 835-845.
65. McDermott, S.P., et al., *Comparison of human cord blood engraftment between immunocompromised mouse strains.* Blood, 2010. **116**(2): p. 193-200.
66. Brehm, M.A., et al., *Parameters for establishing humanized mouse models to study human immunity: analysis of human hematopoietic stem cell engraftment in three immunodeficient strains of mice bearing the IL2rgamma(null) mutation.* Clin Immunol, 2010. **135**(1): p. 84-98.
67. Shultz, L.D., F. Ishikawa, and D.L. Greiner, *Humanized mice in translational biomedical research.* Nat Rev Immunol, 2007. **7**(2): p. 118-30.
68. Ito, A., et al., *Defucosylated anti-CCR4 monoclonal antibody exercises potent ADCC-mediated antitumor effect in the novel tumor-bearing humanized NOD/Shi-scid, IL-2Rgamma(null) mouse model.* Cancer Immunol Immunother, 2009. **58**(8): p. 1195-206.
69. King, M.A., et al., *Human peripheral blood leucocyte non-obese diabetic-severe combined immunodeficiency interleukin-2 receptor gamma chain gene mouse model of xenogeneic graft-versus-host-like disease and the role of host major histocompatibility complex.* Clin Exp Immunol, 2009. **157**(1): p. 104-18.
70. Shultz, L.D., et al., *Humanized mice for immune system investigation: progress, promise and challenges.* Nat Rev Immunol, 2012. **12**(11): p. 786-98.
71. Shimizu, S., et al., *A highly efficient short hairpin RNA potently down-regulates CCR5 expression in systemic lymphoid organs in the hu-BLT mouse model.* Blood, 2010. **115**(8): p. 1534-44.
72. Vatakis, D.N., et al., *Using the BLT humanized mouse as a stem cell based gene therapy tumor model.* J Vis Exp, 2012(70): p. e4181.
73. Onoe, T., et al., *Human natural regulatory T cell development, suppressive function, and postthymic maturation in a humanized mouse model.* J Immunol, 2011. **187**(7): p. 3895-903.
74. Stoddart, C.A., et al., *Superior human leukocyte reconstitution and susceptibility to vaginal HIV transmission in humanized NOD-scid IL-2Rgamma(-/-) (NSG) BLT mice.* Virology, 2011. **417**(1): p. 154-60.

75. Ito, M., et al., *NOD/SCID/gamma(c)(null) mouse: an excellent recipient mouse model for engraftment of human cells.* Blood, 2002. **100**(9): p. 3175-82.
76. Traggiai, E., et al., *Development of a human adaptive immune system in cord blood cell-transplanted mice.* Science, 2004. **304**(5667): p. 104-7.
77. Ishikawa, F., et al., *Development of functional human blood and immune systems in NOD/SCID/IL2 receptor {gamma} chain(null) mice.* Blood, 2005. **106**(5): p. 1565-73.
78. Strowig, T., et al., *Human NK cells of mice with reconstituted human immune system components require preactivation to acquire functional competence.* Blood, 2010. **116**(20): p. 4158-67.
79. Olesen, R., et al., *Immune reconstitution of the female reproductive tract of humanized BLT mice and their susceptibility to human immunodeficiency virus infection.* J Reprod Immunol, 2011. **88**(2): p. 195-203.
80. Denton, P.W., et al., *Generation of HIV latency in humanized BLT mice.* J Virol, 2012. **86**(1): p. 630-4.
81. Vatakis, D.N., et al., *Antitumor activity from antigen-specific CD8 T cells generated in vivo from genetically engineered human hematopoietic stem cells.* Proc Natl Acad Sci U S A, 2011. **108**(51): p. E1408-16.
82. Deng, X., et al., *Synergistic cytotoxicity of ex vivo expanded natural killer cells in combination with monoclonal antibody drugs against cancer cells.* Int Immunopharmacol, 2012. **14**(4): p. 593-605.
83. Luhm, J., et al., *Large-scale generation of natural killer lymphocytes for clinical application.* J Hematother Stem Cell Res, 2002. **11**(4): p. 651-7.
84. Parkhurst, M.R., et al., *Adoptive transfer of autologous natural killer cells leads to high levels of circulating natural killer cells but does not mediate tumor regression.* Clin Cancer Res, 2011. **17**(19): p. 6287-97.
85. Harada, H., et al., *Selective expansion of human natural killer cells from peripheral blood mononuclear cells by the cell line, HFWT.* Jpn J Cancer Res, 2002. **93**(3): p. 313-9.
86. Voskens, C.J., et al., *Ex-vivo expanded human NK cells express activating receptors that mediate cytotoxicity of allogeneic and autologous cancer cell lines by direct recognition and antibody directed cellular cytotoxicity.* J Exp Clin Cancer Res, 2010. **29**: p. 134.
87. Yang, H., et al., *A New Ex Vivo Method for Effective Expansion and Activation of Human Natural Killer Cells for Anti-Tumor Immunotherapy.* Cell Biochem Biophys, 2015. **73**(3): p. 723-9.
88. Chang, Y.H., et al., *A chimeric receptor with NKG2D specificity enhances natural killer cell activation and killing of tumor cells.* Cancer Res, 2013. **73**(6): p. 1777-86.
89. Fujisaki, H., et al., *Replicative potential of human natural killer cells.* Br J Haematol, 2009. **145**(5): p. 606-13.
90. Spanholtz, J., et al., *High log-scale expansion of functional human natural killer cells from umbilical cord blood CD34-positive cells for adoptive cancer immunotherapy.* PLoS One, 2010. **5**(2): p. e9221.
91. Spanholtz, J., et al., *Clinical-grade generation of active NK cells from cord blood hematopoietic progenitor cells for immunotherapy using a closed-system culture process.* PLoS One, 2011. **6**(6): p. e20740.
92. Tam, Y.K., et al., *Ex vivo expansion of the highly cytotoxic human natural killer-92 cell-line under current good manufacturing practice conditions for clinical adoptive cellular immunotherapy.* Cytotherapy, 2003. **5**(3): p. 259-72.

93. Tseng, H.-C., et al., *Induction of Split Anergy Conditions Natural Killer Cells to Promote Differentiation of Stem Cells through Cell-Cell Contact and Secreted Factors.* Frontiers in immunology, 2014. **5**: p. 269-269.